

Quantum Simulations of Lattice Gauge Theories using Ultracold Atoms in Optical Lattices

Erez Zohar

Max-Planck-Institut für Quantenoptik, Hans-Kopfermann-Straße 1, 85748
Garching, Germany.

J. Ignacio Cirac

Max-Planck-Institut für Quantenoptik, Hans-Kopfermann-Straße 1, 85748
Garching, Germany.

Benni Reznik

School of Physics and Astronomy, Raymond and Beverly Sackler Faculty of
Exact Sciences, Tel Aviv University, Tel-Aviv 69978, Israel.

Abstract. Can high energy physics be simulated by low-energy, non-relativistic, many-body systems, such as ultracold atoms? Such ultracold atomic systems lack the type of symmetries and dynamical properties of high energy physics models: in particular, they manifest neither local gauge invariance nor Lorentz invariance, which are crucial properties of the quantum field theories which are the building blocks of the standard model of elementary particles.

However, it turns out, surprisingly, that there are ways to configure atomic system to manifest both local gauge invariance and Lorentz invariance. In particular, local gauge invariance can arise either as an effective, low energy, symmetry, or as an "exact" symmetry, following from the conservation laws in atomic interactions. Hence, one could hope that such quantum simulators may lead to new type of (table-top) experiments, that shall be used to study various QCD phenomena, as the confinement of dynamical quarks, phase transitions, and other effects, which are inaccessible using the currently known computational methods.

In this report, we review the Hamiltonian formulation of lattice gauge theories, and then describe our recent progress in constructing quantum simulation of Abelian and non-Abelian lattice gauge theories in $1 + 1$ and $2 + 1$ dimensions using ultracold atoms in optical lattices.

Contents

1	Introduction: Quantum Simulation of High Energy Physics	4
1.1	Quantum Simulations	4
1.2	Quantum Simulations of High Energy Physics	5
1.3	Proposals for Quantum Simulations of High Energy Physics	7
2	Lattice Gauge Theory: A brief review	8
2.1	Hamiltonian Formulation	9
2.1.1	Hopping fermions and global gauge symmetry.	9
2.1.2	Local Gauge Symmetry.	10
2.1.3	Dynamical Gauge Fields.	11
2.2	Abelian Theories	14
2.2.1	Compact QED (cQED)	14
2.2.2	\mathbb{Z}_N	16
2.3	Non-Abelian Yang-Mills Theories: $SU(2)$ as an example	17
2.4	Physical content of the models	18
2.4.1	Quark Confinement.	18
2.4.2	Strong Coupling Lattice Gauge Theories.	20
2.4.3	The Weak Limit of $cQED$	21
3	Ultracold Atoms in Optical Lattices : A brief review	22
3.1	Generation of an Optical Potential	22
3.2	Multi-species Lattices and Spinor Condensates	24
3.3	Scattering of Ultracold Atoms	25
3.4	Multiple Species Scattering	26
3.5	Summary of the Available Interactions and Possibilities	27
4	A framework for Quantum Simulation of lattice gauge theories with ultracold atoms in optical lattices	29
5	Effective gauge invariance emerging at low energies	30
5.1	cQED in $2 + 1$ dimensions - link interactions	31
5.2	Truncated cQED model - link interactions	32
5.3	Effective Gauge Invariance - some general remarks	35
6	Local gauge invariance arising from many body interaction symmetries	35
6.1	Compact QED - on-link interactions	36
6.2	$SU(2)$ - Yang Mills theory - on-link interactions	37
6.2.1	Left and right Schwinger representations.	37
6.2.2	Truncation scheme for the Hilbert space of non-Abelian groups.	38
6.2.3	Realization of the truncated on-link interactions.	40
6.3	Plaquette interactions: $d + 1$ dimensional Abelian and non-Abelian theories	43
6.4	Gauge invariance from atomic interaction symmetries - some general remarks	44

<i>CONTENTS</i>	3
7 Discussion	45
7.1 Advantages of quantum simulation over other approaches	46
7.2 Simulated models	47
7.3 Open problems	47
7.4 Summary	48

1. Introduction: Quantum Simulation of High Energy Physics

1.1. Quantum Simulations

Quantum simulation [1] is a relatively new physical field, concerning the simulation of quantum systems with other quantum systems. The original idea goes back to Richard Feynman [2], who argued that since nature is quantum, it should be simulated by quantum computers. However, it was "left aside" for about two decades, as no candidates for playing the role "quantum simulators" were available. Following Feynman's pioneering work [2], it has been shown that universal quantum computers [3, 4] could in principle simulate general many-body systems [5] as well as quantum fields [6], serving as digital quantum simulators.

Thanks to the enormous progress carried out over the last decades on the road towards "Universal Quantum Computers", several quantum systems are now highly and precisely controllable in the laboratory, mainly belonging to atomic physics and quantum optics. These are, for example, ultracold atoms in optical lattices [7, 8, 9, 10, 11], including Bose-Einstein condensates; Trapped ions [12, 13, 14, 15, 16]; photonic systems [17], Rydberg Atoms [18] and more. Thus, although a full-fledged, universal quantum computer has not been realized yet, one may utilize these systems in order to create *analog quantum simulators*, which are indeed non-universal simulators, but nevertheless, allow for quantum simulation of quantum systems. This is done by mapping the degrees of freedom of the simulated systems into those of the controllable simulating system. Such quantum simulators provide simple realizations for quantum models and phenomena which may be, otherwise, inaccessible, either theoretically, experimentally, or numerically, amendable for direct observation of many-body physics phenomena. Using such simulators, one could study, experimentally, the spectrum and dynamics of the simulated system, and therefore these simulators may be regarded as analog quantum computers, specifically tailored to the simulated systems. Quantum simulation also has the possibility of realizing physical models which are "unreal" - not believed to be found in nature.

One could also propose and realize *digital quantum simulators*, which fulfill the same tasks, but using quantum computation methods of qubits and quantum gates. This work, however, deals with analog simulations.

Thus, quantum simulation is currently a rapidly growing physical area, involving multidisciplinary research, both theoretical and experimental. The theoretical research focuses on mapping the simulated physics into the quantum simulating systems, considering possible realizations and required approximations of the simulated model, as well as methods to control and get the most out of the simulating systems. Hence the multidisciplinary nature: it involves both the simulated and the simulating physics, which may belong to two totally different physical disciplines, at least from a traditional perspective. The experimental research focuses on improving the capabilities and controllability of the simulating systems, also by developing new techniques and simulating systems, and of course, on realizing quantum simulations, serving as table-top experiments, with great success.

Having been realized using AMO physics, models of Condensed Matter and statistical mechanics are the natural candidates for quantum simulations. These may be Hubbard models, spin chains and Heisenberg models and others - only few examples are [7, 19, 20, 21, 22, 23, 24, 25, 26, 27, 28, 29, 30]. Effects of artificial, external gauge potentials, experienced by cold atoms, have also been considered

for quantum simulation, among more topological effects, such as the Aharonov-Bohm effect, Berry's phase, topological insulators and the quantum Hall effect [31, 32, 26, 33, 34, 35, 36, 37, 38, 39, 40, 41, 42]. A significant example to the power of quantum simulation in condensed matter physics is the experiment for simulating the phase transition in Hubbard models [20].

However, quantum simulations are not limited only to condensed matter physics, and they involve also other physical areas, such as gravity, including Black-Hole Hawking [43] and Unruh [44] radiation [45, 46, 47, 48, 49, 50, 51, 52, 53]. Relativistic physics has been considered as well, including, for example, Dirac Equation (including Zitterbewegung and the Klein paradox) [54, 55, 56, 57], the famous Fermi two-atom problem [58, 59], neutrino oscillations [60] and the Majorana equation [61, 62]. The next obvious step is to consider quantum field theories as well.

Quantum simulations of quantum field theories involve these of vacuum entanglement of a scalar field [63, 64] as well as the interacting scalar-fermionic theories of Thirring and Gross-Neveu [65]. Fermions in lattice gauge theories have been considered as well, for example in the quantum simulations of Axions and Wilson fermions [66], Dirac fields in curved spacetime [67], general simulations of QFT with topological insulators [68] and Schwinger's pair-creation mechanism [69]. Simulations of nontrivial geometries and topologies and extra dimensions, using internal degrees of freedom [70, 71] have been suggested too, as well as simulations of some supersymmetric theories, such as [72, 73, 74].

1.2. Quantum Simulations of High Energy Physics

Another class of quantum simulations is those of high energy physics (HEP), which involve dynamical gauge fields.

Gauge fields are in the core of the standard model of particle physics [75, 76]. These fields, through their local symmetry, induce the interactions among matter particles, which are fermions - or, phrased differently, the excitations of the gauge fields are the so called gauge bosons, force carriers, or interaction mediators. (In the current report, we shall not discuss the Brout-Englert-Higgs mechanism [77, 78], which introduces a scalar field, not playing the role of a gauge field.)

Each gauge theory is based on local gauge invariance - invariance to local gauge transformations, generated by the so called *gauge group*. Such groups may be either Abelian or non-Abelian: for example, *QED* (Quantum Electrodynamics) is an Abelian gauge theory, based on the group $U(1)$, while the strong interactions are described by the theory of *QCD* (Quantum Chromodynamics), which has the non-Abelian local gauge symmetry of $SU(3)$. These symmetries induce the interactions among matter particles, which have different *gauge charges* - the electric charge in *QED*, or the non-Abelian color charge in *QCD*, for example. In the case of non-Abelian groups, the gauge bosons (e.g., *QCD*'s gluons) also carry charge of their own, unlike the Abelian photons of *QED*.

The standard model of particle physics involves a local gauge symmetry of $SU(3) \times SU(2) \times U(1)$, corresponding to the strong (*QCD*), weak and electromagnetic (*QED*) interactions respectively. All the gauge groups in this case are continuous groups - Yang-Mills theories [79].

The study of gauge theories, within and beyond the framework of the standard model, employs many theoretical techniques. These include, of course, the perturbative approach of Feynman diagrams [80, 81, 82, 83, 84], which has been

applied with great success to quantum electrodynamics. However, within QCD , such perturbative methods face a problem. In high energies, or short distances (such as the scale of deep inelastic scattering) perturbative techniques work fairly well, since, due to asymptotic freedom [85] (and the earlier results of the parton model and Bjorken scaling [86, 87]), in this regime the quarks behave essentially as free, pointlike particles (within the hadrons). On the other hand, at low energies, or large distances, the quarks are subject to the so-called *quark confinement* [88] which forbids the existence of free quarks and rather binds them together into composite particles - hadrons. This limit is nonperturbative, and other techniques must be applied in order to study it.

The most powerful approach that has been developed for non-perturbative QCD effects is lattice gauge theory [88, 89, 90]. It allows probing and calculating many important quantities and phenomena of the theory, both analytically, as the lattice suggests a regularization method, and numerically, mostly using Monte-Carlo classical simulation methods. Such studies have led to significant and remarkable results, such as the low-energy spectrum of QCD and the CKM matrix elements [91], several results concerning the quark-gluon plasma [92, 93, 94, 95] and the deconfinement phase transition at finite temperature [96, 97, 98] - just to name a few.

Monte Carlo calculations, nevertheless, are limited in certain important case. For example - the computationally hard sign problem [99] that limits calculations in regimes with a finite chemical potential for the fermions - which is problematic, for example, for the study of the QCD phases of color-superconductivity or quark-gluon plasma [94, 100, 101], or the fact that the Monte-Carlo calculations are of Euclidean correlation functions, and not of real-time dynamics. Indeed a full study of quark confinement with dynamical charges, and other nonperturbative phenomena in QCD in 3+1 dimensions is still lacking.

Another successful avenue for the exploration of such theories has been the development of "toy models" - simpler physical theories which capture the essential physics in question. Such studies include, for example, confinement in Abelian theories in various dimensions (including on the lattice) [102, 103, 104, 105, 88, 89, 106, 107, 108, 109], or QCD_2 , the 1+1 dimensional version of Quantum Chromodynamics, which has been a target of interest over the last decades, as a natural playground for nonperturbative calculations, and as a basis for analytical understanding of real-world, 3+1 QCD (QCD_4). There, several nonperturbative methods have been proven fruitful and useful for derivation of the spectrum of $SU(N_c)$ theories. First, in the large N_c limit, firstly discussed (and solved) by 't Hooft [110, 111], where the mesonic spectrum of the theory is revealed, manifesting confinement of quarks. Other methods to study the hadronic spectrum of QCD_2 have been DLCQ (discretized light-cone quantization) [112] and current algebras [113]. Witten's non-Abelian bosonization [114] has helped to gain insight on the strong coupling Baryonic spectrum and quark content [115, 116, 117, 118]. The relation of the fermion mass with confinement in these theories has been studied, for example, in [119, 120].

Thus, new methods of calculations in gauge theories, in particular QCD , could be of a great help. Quantum simulation methods may be candidates for that. Once a quantum simulator for a gauge theory is built, one could use it to observe, experimentally, the otherwise inaccessible physics of these special, nonperturbative regimes. Such quantum simulators may be the quantum computers of HEP calculations: allowing for real-time dynamics and including real fermions rather than Grassman variables, suffering from the sign-problem, they suggest a way to overcome the problems of numerical lattice gauge theories mentioned above. Besides

that, reconstructing the standard model (in this case, out of atomic building blocks), or any of its sub-models, could help in understanding the basic interactions and symmetries of the theory.

Quantum simulation of high energy physics, involving gauge field(s), may be both theoretically and experimentally harder than simulating other physical phenomena, in condensed matter physics, for example. In fact, three basic requirements [121] must be met in order to obtain a quantum simulator of a gauge theory: the simulation must include *both fermionic and bosonic degrees of freedom* (matter and gauge fields/particles); It must have a *Relativistic, Lorentz invariance* (a causal structure); and it must involve *local gauge invariance*, in order to obtain conservation of charges, and of course - the required interactions. These requirements are not trivially met, however, they must be satisfied, as without them, the theories in question could not be achieved. As we show in this paper, these requirements may be satisfied and fulfilled in certain configurations of atomic systems.

1.3. Proposals for Quantum Simulations of High Energy Physics

So far, only theoretical proposals have been suggested for quantum simulations of high energy physics.

The first group of works contains condensed matter systems in which gauge invariance emerges, which may serve as quantum simulators for Abelian gauge theories. These include, for example, an effective emergence of a $U(1)$ spin liquid in Pyrochlore [122]; A ring exchange model using molecular states in optical lattices, yielding a Coulomb phase $U(1)$ in the limit of no hopping [123]; The effective emergence of artificial photons in dipolar bosons in an optical lattice [124]; a *digital* quantum simulation of spin- $\frac{1}{2}$ $U(1)$ gauge theory, as a low energy theory of Rydberg atoms [18]; and the emergence of gauge fields out of time reversal symmetry breaking for spin- $\frac{5}{2}$ in honeycomb optical lattices [125].

Quantum simulation, using ultracold atoms in an optical lattice, of continuous QED has been suggested in [126]. However, most of the works so far concentrate on quantum simulations of lattice gauge theories, which are more suited for quantum simulation using optical lattices.

Simulations of pure-gauge compact QED ($cQED$, see section 2.2.1) include a simulation of the Kogut-Susskind Hamiltonian in 2+1 dimensions using Bose-Einstein condensates in optical lattices [127], as well as a simulation of a truncated, spin-gauge model, using single atoms in optical lattices [128].

Simulations of $U(1)$ models with matter have been suggested as well - either for an Abelian link model [129, 130, 131] - a 1+1 dimensional simulation of the lattice link Schwinger model [132], or a generalization of the spin-gauge approach, to include dynamical fermions in 2+1 dimensions [133]. The above proposals for $cQED$ simulations with ultracold atoms introduce gauge invariance as an effective symmetry, by constraining Gauss's law in the Hamiltonian, with a large energy penalty. Another approach for simulation, utilizing fundamental symmetries of the ultracold atoms, is proposed in [121], for 1+1 and 2+1 dimensional $cQED$, with or without dynamical matter.

Recent proposals for such simulations also utilize other systems - such as superconducting quantum circuits [134, 135] and trapped ions [136], both simulating the Abelian link model. A digital simulation of a $U(1)$ gauge theory is presented in [137], using Rydberg atoms.

Simulations of discrete lattice gauge theories have been suggested as well, including discrete Abelian (\mathbb{Z}_N) and non-Abelian (D_N) models using arrays of Josephson junctions [138], a digital simulation of \mathbb{Z}_2 with Rydberg atoms [137] and an analog simulation of \mathbb{Z}_N , with an explicit construction for \mathbb{Z}_3 in an optical lattice [121]. A way to truncate the Hilbert space of a $U(1)$ theory in a manner similar to \mathbb{Z}_N was proposed in [139].

Quantum simulations of Non-Abelian gauge theories with continuous groups ($SU(2)$ Yang Mills models, with possible generalizations to $U(N), SU(N)$) have been proposed too - Analog simulations with cold atoms utilizing prepotentials [140, 141, 142, 143] or rishons in the link model [144, 145] have been suggested in [146] and [147] respectively, where the first utilizes hyperfine angular momentum conservation to obtain local gauge invariance, and the latter starts with a larger symmetry group, which must be broken. A digital simulation of an $SU(2)$ gauge magnet [130, 148] has been suggested in [149], while a digital quantum simulation of an $SU(2)$ link model with triangular plaquettes, using superconducting qubits, has been suggested in [150]. A new way for imposing gauge invariance using dissipation (Zeno effect), with an explicit construction for a non-Abelian model, has been given in [151].

In general, the dimensions of the analog quantum simulations with optical lattices are restricted only by experimental and technological considerations. Thus, the above suggestions for $2 + 1$ dimensional systems, using optical lattices, should apply, in principle, also to $d + 1$ systems, given, of course, that the required technological challenge is met. The $1 + 1$ quantum simulations mentioned above which use optical lattices may be generalized to further dimensions but, mostly, without the magnetic (plaquette) terms, and thus are simply quantum simulations the strong limit of lattice gauge theories (see section 2 for an explanation of these terms). For other simulating systems and/or digital simulations, the case may be different, due to possible dimension-dependent properties of the simulating system.

For a comprehensive review on the recent progress in quantum simulation proposals of link-Rishon models, the reader should refer to [152].

Throughout this work, $\hbar = c = 1$, and the Einstein summation convention is assumed.

2. Lattice Gauge Theory: A brief review

Lattice gauge theories [89, 90, 153, 154, 155, 156] are formulations of gauge theories on a discretized space, or spacetime. They were originally invented by Wilson, as a tool for the study of the quark confinement problem [88]. It is an important tool in high energy physics, and especially in *QCD* (Quantum Chromodynamics - the theory of the strong interactions) as it allows performing nonperturbative calculations (numerically, using Monte-Carlo methods) and thus provides insights into the perturbatively-inaccessible regions of *QCD*, due to the running coupling.

Besides addressing the confinement of quarks (or charges in analogous Abelian theories, as will be later discussed), lattice gauge theories have enabled the computation of other important quantities in *QCD*, such as the hadronic structure and spectrum, as may be read in the reviews [90, 101, 91] and many others.

In the following review of lattice gauge theory, we follow the Hamiltonian (canonical), Kogut-Susskind formulation of lattice gauge theories [157, 89, 90] (rather than the more "conventional" Euclidean approach). This is since the Hamiltonian

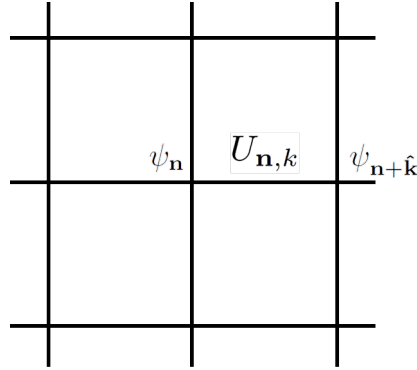


Figure 1. The lattice structure. The gauge degrees of freedom occupy the links, whereas the fermionic matter - the vertices.

language is much more natural in the context of atomic and optical physics, used for the simulating systems.

2.1. Hamiltonian Formulation

2.1.1. Hopping fermions and global gauge symmetry. Consider fermions on a d dimensional spatial lattice, with nearest-neighbor hopping. The Hamiltonian takes the form

$$H = \sum_{\mathbf{n}} M_{\mathbf{n}} \psi_{\mathbf{n}}^{\dagger} \psi_{\mathbf{n}} + \epsilon \sum_{\mathbf{n},k} (\psi_{\mathbf{n}}^{\dagger} \psi_{\mathbf{n}+\hat{\mathbf{k}}} + h.c.) \quad (1)$$

where $\mathbf{n} \in \mathbb{Z}^d$ label the lattice’s vertices and $k \in \{1, \dots, d\}$ labels the lattice’s directions; $\hat{\mathbf{k}}$ is a unit vector (where the lattice spacing is $a = 1$) in the k th direction. The Hamiltonian consists of local “mass” terms and hopping terms (see figure 1).

$\psi_{\mathbf{n}}$ are spinors of some unitary gauge group G , in some representation r \ddagger . For example, $\psi_{\mathbf{n}}$ are merely fermionic annihilation operators in the case $G = U(1)$. For $G = SU(N)$, in the fundamental representation, these are N -component spinors, containing N annihilation operators:

$$\psi_{\mathbf{n}} = \begin{pmatrix} \psi_{\mathbf{n},1} \\ \psi_{\mathbf{n},2} \\ \vdots \\ \psi_{\mathbf{n},N} \end{pmatrix} \quad (2)$$

where in Hamiltonian (1), and in what follows, summation on the *group* indices is assumed, e.g.

$$\psi_{\mathbf{n}}^{\dagger} \psi_{\mathbf{n}} \equiv \sum_i \psi_{\mathbf{n},i}^{\dagger} \psi_{\mathbf{n},i} \quad (3)$$

The Hamiltonian (1) is invariant under *global gauge transformations* of the gauge group G . That means, that if we pick some group element $V \in G$ (which is unitary)

\ddagger Note that we only consider here the *gauge* degrees of freedom; Each component of these gauge spinors may also be a spinor in terms of the spin or flavor degrees of freedom, but we disregard it here.

and perform the transformation

$$\psi_{\mathbf{n}} \longrightarrow V\psi_{\mathbf{n}} \quad ; \quad \psi_{\mathbf{n}}^{\dagger} \longrightarrow \psi_{\mathbf{n}}^{\dagger}V^{\dagger} \quad (4)$$

the Hamiltonian is left intact §. This corresponds to a conservation of the total number of fermions,

$$N_{tot} = \sum_{\mathbf{n}} \psi_{\mathbf{n}}^{\dagger}\psi_{\mathbf{n}} \quad (5)$$

which is obvious, as all the terms of the Hamiltonian annihilate one fermion and create another one.

2.1.2. Local Gauge Symmetry. Next, let us lift the symmetry to be local, by generalizing the transformation to

$$\psi_{\mathbf{n}} \longrightarrow V_{\mathbf{n}}\psi_{\mathbf{n}} \quad ; \quad \psi_{\mathbf{n}}^{\dagger} \longrightarrow \psi_{\mathbf{n}}^{\dagger}V_{\mathbf{n}}^{\dagger} \quad (6)$$

- i.e., each vertex is assigned *locally* a unitary element of the gauge group. The mass terms of (1) are local and hence remain intact, but the hopping terms vary under the transformation, for example

$$\psi_{\mathbf{n}}^{\dagger}\psi_{\mathbf{n}+\hat{\mathbf{k}}} \longrightarrow \psi_{\mathbf{n}}^{\dagger}V_{\mathbf{n}}^{\dagger}V_{\mathbf{n}+\hat{\mathbf{k}}}V_{\mathbf{n}+\hat{\mathbf{k}}}\psi_{\mathbf{n}+\hat{\mathbf{k}}} \quad (7)$$

The gauge symmetry will be restored if we introduce a connection $U_{\mathbf{n},k}$, located on the link emanating from the vertex \mathbf{n} in the k th direction. $U_{\mathbf{n},k}$ is an element of the gauge group in the appropriate representation (corresponding to the spinors to which it is coupled), a unitary operator \parallel undergoing the gauge transformation as

$$U_{\mathbf{n},k} \longrightarrow V_{\mathbf{n}}U_{\mathbf{n},k}V_{\mathbf{n}+\hat{\mathbf{k}}}^{\dagger} \quad (8)$$

then, if the Hamiltonian is changed to

$$H_{GM} = \sum_{\mathbf{n}} M_{\mathbf{n}}\psi_{\mathbf{n}}^{\dagger}\psi_{\mathbf{n}} + \epsilon \sum_{\mathbf{n},k} (\psi_{\mathbf{n}}^{\dagger}U_{\mathbf{n},k}\psi_{\mathbf{n}+\hat{\mathbf{k}}} + h.c.) \quad (9)$$

the gauge invariance is, indeed, restored, and the gauge transformation leaves it intact. The name H_{GM} stands for the gauge-matter interactions described by it.

We denote the local gauge transformation generators by $G_{\mathbf{n}}^i$. Due to the gauge symmetry, they commute with the Hamiltonian,

$$[H, G_{\mathbf{n}}^i] = 0 \quad (10)$$

and thus the physical Hilbert space \mathcal{H} is also gauge-invariant, i.e. divided into sectors of eigenvalues of $G_{\mathbf{n}}^i$ (see figure 2):

$$\mathcal{H} = \bigoplus_{\{q_{\mathbf{n}}^i\}} \mathcal{H}(\{q_{\mathbf{n}}^i\}) \quad (11)$$

§ The group element V in (4) is, of course, written in the appropriate representation (the same as the spinors). However, note that the equation is representation independent. When a representation is chosen it must be identical for the spinor and the group element.

∥ The unitarity has many advantages and is used in the context of conventional, Wilsonian minimally-coupled lattice gauge theories. However, the transformation (symmetry) properties may be satisfied if the operator is not unitary as well, as we do in our simulations [128, 133, 121, 146].

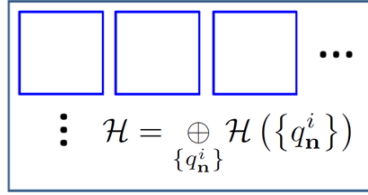


Figure 2. The physical Hilbert space of a gauge invariant theory is divided into separate sectors, corresponding to different static charge configurations (11), represented by boxes. The gauge invariant dynamics does not mix among them (13). These are two consequences of gauge invariance (10).

Each such sector $\mathcal{H}(\{q_n^i\})$ has a set of eigenvalues $\{q_n^i\}$, called *static charges*, such that for every $|\psi(\{q_n^i\})\rangle \in \mathcal{H}(\{q_n^i\})$,

$$G_n^i |\psi(\{q_n^i\})\rangle = q_n^i |\psi(\{q_n^i\})\rangle \quad (12)$$

Note that as the generators do not commute for a non-Abelian group (this shall be clear in the following subsection, where they are explicitly defined). The static charges, thus, can only be defined by the eigenvalues of a subset of some commuting operators. The above equation is the generalized *Gauss's Law*, and the dynamics does not mix these sectors, i.e.

$$\langle \psi(\{p_n^i\}) | H | \psi(\{q_n^i\}) \rangle \propto \prod_n \delta_{p_n^i, q_n^i} \quad (13)$$

2.1.3. Dynamical Gauge Fields. We shall identify the connections $U_{\mathbf{n},\mathbf{k}}$ with the gauge group elements, i.e. introduce the group parameters $\theta_{\mathbf{n},k}^i$ - Hermitian operators, such that in a given representation r , with the matrix representation of the group generators $T_i^{(r)}$,

$$U_{\mathbf{n},k}^{(r)} = e^{i\theta_{\mathbf{n},k}^i T_i^{(r)}} \quad (14)$$

where a summation on the group indices i is implicit. We shall assume next working in the fundamental representation (generalizations to other representations are straightforward), and disregard the representation indices in this case: $U_{\mathbf{n},k} = e^{i\theta_{\mathbf{n},k}^i T_i}$.

One could then define operators which are conjugate to the group parameters, to serve as generalized momenta. In case of the Abelian group $U(1)$, where $U_{\mathbf{n},k} = e^{i\theta_{\mathbf{n},k}}$, one could define the conjugate momentum to be proportional simply to $\dot{\theta}_{\mathbf{n},\mathbf{k}}$. But generally, when G may be non-Abelian, one must pay attention of the non-commutativity of the group in doing that. Thus, we could reformulate the Abelian case and define the conjugate momentum there as

$$L_{\mathbf{n},k} = -i\dot{U}_{\mathbf{n},k} U_{\mathbf{n},k}^\dagger = -iU_{\mathbf{n},k}^\dagger \dot{U}_{\mathbf{n},k} \quad (15)$$

The differential representation would be

$$L_{\mathbf{n},k} = -i \frac{\partial}{\partial \theta_{\mathbf{n},k}} \quad (16)$$

from which the canonical commutation relation

$$[\theta_{\mathbf{n},k}, L_{\mathbf{n},k}] = i \quad (17)$$

results, and from which, as it is the generator of angular translations,

$$[L_{\mathbf{n},k}, U_{\mathbf{n},k}] = U_{\mathbf{n},k} \quad (18)$$

Thus a reasonable choice for the dynamic part of the gauge field would be

$$H_E^{ab} \propto \sum_{\mathbf{n},k} L_{\mathbf{n},k}^2 \quad (19)$$

in agreement with the Abelian version of the Kogut-Susskind Hamiltonian (see below).

Let us now generalize it for non-Abelian groups [158]. Due to the non-Abelian nature of the group, one could define two sets of such operators, left and right -

$$L_{\mathbf{n},k} = -i\dot{U}_{\mathbf{n},k}U_{\mathbf{n},k}^\dagger \quad ; \quad R_{\mathbf{n},k} = -iU_{\mathbf{n},k}^\dagger\dot{U}_{\mathbf{n},k} \quad (20)$$

(for an Abelian group $L = R$, but this does not hold in general). One can expand these operators in terms of the group's representation matrices,

$$L_{\mathbf{n},k} = L_{\mathbf{n},k}^i T_i \quad ; \quad R_{\mathbf{n},k} = R_{\mathbf{n},k}^i T_i \quad (21)$$

and then construct the differential forms of the operators $\{L_{\mathbf{n},k}^a\}, \{R_{\mathbf{n},k}^a\}$. These operators are called *left and right* generators of the group, since they satisfy the group's algebra \mathfrak{A} ,

$$[L_{\mathbf{n},k}^i, U_{\mathbf{n},k}] = T_i U_{\mathbf{n},k} \quad (22)$$

$$[R_{\mathbf{n},k}^i, U_{\mathbf{n},k}] = U_{\mathbf{n},k} T_i \quad (23)$$

$$[L_{\mathbf{n},k}^i, L_{\mathbf{n},k}^j] = -if_{ijl}L_{\mathbf{n},k}^l \quad (24)$$

$$[R_{\mathbf{n},k}^i, R_{\mathbf{n},k}^j] = if_{ijl}L_{\mathbf{n},k}^l \quad (25)$$

$$[L_{\mathbf{n},k}^i, R_{\mathbf{n},k}^j] = 0 \quad (26)$$

where $\{T_i\}$ are the group's generators and f_{ijl} are the group's structure constants⁺. Generators and group elements from different links commute, of course.

Note that due to the definition (20), one could prove that

$$R_{\mathbf{n},k} = U_{\mathbf{n},k}^\dagger L_{\mathbf{n},k} U_{\mathbf{n},k} \quad (27)$$

and thus if we calculate the trace in group space we find out that

$$\text{tr}(R_{\mathbf{n},k}^2) = \text{tr}(L_{\mathbf{n},k}^2) \quad (28)$$

\blacklozenge Note that the right and left operators may be defined in other conventions as well, resulting in different signs in the group's algebra.

⁺ In a general representation r , these equations would be generalized in a straightforward manner, e.g. $[L_{\mathbf{n},k}^i, U_{\mathbf{n},k}^{(r)}] = T_i^{(r)} U_{\mathbf{n},k}^{(r)}$, where $T_i^{(r)}$ stands for the matrix representation of the generator in r , and $U_{\mathbf{n},k}^{(r)}$ stands for the matrix representation of the group element. If one wishes to explicitly write the group's indices, the equations will look like, for example, $[L_{\mathbf{n},k}^i, (U_{\mathbf{n},k})_{jl}] = (T_i U_{\mathbf{n},k})_{jl}$

This can be reformulated using the generators,

$$\sum_i (R_{\mathbf{n},k}^i)^2 = \sum_i (L_{\mathbf{n},k}^i)^2 \equiv \mathbf{L}_{\mathbf{n},k}^2 \quad (29)$$

giving us the electric part of the non-Abelian Kogut-Susskind Hamiltonian,

$$H_E \propto \sum_{\mathbf{n},k} \mathbf{L}_{\mathbf{n},k}^2 \quad (30)$$

We can refer to $\{L_{\mathbf{n},\hat{\mathbf{k}}}^i\}, \{R_{\mathbf{n},\hat{\mathbf{k}}}^i\}$ as the left and right electric fields, conjugate (in some sense) to the vector potential. Their difference along a link corresponds to the charge carried by it: no charge in the Abelian case, and the color charge in the $SU(N)$ case.

The gauge transformation generators are then given by [157]

$$G_{\mathbf{n}}^i = \sum_k \left(L_{\mathbf{n},k}^i - R_{\mathbf{n}-\hat{\mathbf{k}},k}^i \right) - Q_{\mathbf{n}}^i \quad (31)$$

where $Q_{\mathbf{n}}^a$ is the *dynamical* charge, which will be introduced later.

The Abelian version of the generator is merely

$$\begin{aligned} G_{\mathbf{n}} &= \sum_k \left(L_{\mathbf{n},k} - L_{\mathbf{n}-\hat{\mathbf{k}},k} \right) - Q_{\mathbf{n}} \\ &\equiv \text{div}_{\mathbf{n}} L_{\mathbf{n},k} - Q_{\mathbf{n}} \end{aligned} \quad (32)$$

in which the discrete divergence is defined, and from which the relation to Gauss's law is obvious.

One would also like to consider a gauge-field self interaction. Gauge invariance forces us to consider only group traces of products of group elements along close paths. The smallest such interactions are the so-called *plaquette* terms, involving unit squares of the lattice, from which we obtain the magnetic part of the Kogut-Susskind Hamiltonian [157]

$$H_B \propto \sum_{\text{plaquettes}} \left(\text{tr} \left(U_1 U_2 U_3^\dagger U_4^\dagger \right) + h.c. \right) \quad (33)$$

with the group elements usually in the fundamental representation (even if there are charges in other representation which requires the use of other representations when coupling them to the gauge field) which simplifies in the Abelian case to [89]

$$H_B^{ab} \propto \sum_{\text{plaquettes}} \cos(\theta_1 + \theta_2 - \theta_3 - \theta_4) \quad (34)$$

where the numbers in both the equations are according to the plaquette convention presented in figure 3. Note that this agrees with the terms of the Wilson action [88], and thus with the ‘‘usual’’ procedure of obtaining the Hamiltonian (by a Legendre transformation of the Lagrangian).

We have obtained the terms of the Kogut-Susskind Hamiltonian only up to some proportion factors. One can find them by taking the (classical) continuum limit. Doing that (or using a Legendre transformation of the Lagrangian) one obtains the Kogut-Susskind Hamiltonian

$$H_{KS} = \frac{1}{2} g^2 \sum_{\mathbf{n},k} \mathbf{L}_{\mathbf{n},k}^2 - \frac{1}{2g^2} \sum_{\text{plaquettes}} \left(\text{tr} \left(U_1 U_2 U_3^\dagger U_4^\dagger \right) + h.c. \right) \quad (35)$$

where g is the coupling constant.

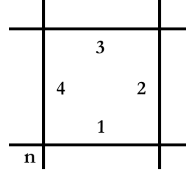


Figure 3. The convention of numbering the links in plaquette interactions (see equations (33),(34)).

2.2. Abelian Theories

2.2.1. Compact QED (cQED) The first theory we shall consider is Compact Quantum Electrodynamics - cQED [89]. This theory's continuum limit is Quantum Electrodynamics (QED). Its lattice version is compact, involving angular variables.

This is an Abelian, continuous gauge theory, with the gauge group $U(1)$. Thus, the group elements are simply unitary phases

$$U_{\mathbf{n},k} = e^{i\theta_{\mathbf{n},k}} \tag{36}$$

as we have already discussed, $\theta_{\mathbf{n},k}$ are analogous to the vector-potential, and the conjugate momenta are $L_{\mathbf{n},k} = -i \frac{\partial}{\partial \theta_{\mathbf{n},k}} - U(1)$ (planar) angular momentum operators. The canonical commutation relation $[\theta_{\mathbf{n},k}, L_{\mathbf{n},k}] = i$ ensures that $U_{\mathbf{n},k}$ is a raising operator of the electric field $[L_{\mathbf{n},k}, U_{\mathbf{n},k}] = U_{\mathbf{n},k}$, and $U_{\mathbf{n},k}^\dagger$ is the lowering operator, both are unitary.

The Kogut-Susskind Hamiltonian takes the form

$$H_{KS} = \frac{g^2}{2} \sum_{\mathbf{n},k} L_{\mathbf{n},k}^2 - \frac{1}{g^2} \sum_{\text{plaquettes}} \cos(\theta_1 + \theta_2 - \theta_3 - \theta_4) \tag{37}$$

where the indices inside the plaquette term are with respect to the convention of figure 3. Also note that the argument of the cosine corresponds to the lattice curl, manifesting that the continuum limit of this term gives rise to the magnetic energy.

Let us consider the local Hilbert space on each link. One could work in the basis of electric (flux) eigenstates, which is a good basis in the strong coupling limit $g^2 \gg 1$, as shall be discussed when we consider confinement. The eigenstates of L on a single link satisfy

$$L|m\rangle = m|m\rangle \tag{38}$$

where m takes any integer value, either positive or negative. In coordinate (angle) representation, the wavefunctions are

$$\phi_m(\theta) = \langle \theta|m\rangle = \frac{1}{\sqrt{2\pi}} e^{im\theta} \tag{39}$$

The Abelian Gauss's law takes the form

$$\begin{aligned} G_{\mathbf{n}} &= \sum_k \left(L_{\mathbf{n},k} - L_{\mathbf{n}-\hat{\mathbf{k}},k} \right) - Q_{\mathbf{n}} \\ &\equiv \text{div}_{\mathbf{n}} L_{\mathbf{n},k} - Q_{\mathbf{n}} \end{aligned} \tag{40}$$

and thus, in this basis, the gauge-invariant states satisfy (without dynamical matter)

$$G_{\mathbf{n}} |\phi\rangle = \sum_k \left(m_{\mathbf{n},k} - m_{\mathbf{n}-\hat{\mathbf{k}},k} \right) |\phi\rangle = q_{\mathbf{n}} |\phi\rangle \quad (41)$$

where $q_{\mathbf{n}}$ is the (C-number) static charge.

What are the interactions?

- (i) The plaquette interaction, in this language, changes the electric flux on a plaquette, such that in two links the flux increases by a single unit, and in the other two it is lowered. This is done only in two possible orientations, which are the only possibilities which leave the eigenvalue of $G_{\mathbf{n}}$ intact in all the four vertices of each plaquette - thus, this is the “physical interpretation” of the commutativity of the plaquette interactions with Gauss’s law.
- (ii) If we wish to introduce dynamical charges, staggered [157, 159], for example *, with a Hamiltonian of the form

$$H_M = \epsilon \sum_{\mathbf{n},k} \left(\psi_{\mathbf{n}}^\dagger e^{i\theta_{\mathbf{n},k}} \psi_{\mathbf{n}+\hat{\mathbf{k}}} + H.c. \right) + m \sum_{\mathbf{n}} (-1)^{\sum_k n_k} \psi_{\mathbf{n}}^\dagger \psi_{\mathbf{n}} \quad (42)$$

where $\{n_k\}$ are the indices of the vertex \mathbf{n} . we may interpret the gauge invariant interactions as ones which raise the dynamical charge on one edge of the link, lower it on the other side, and raise/lower the electric flux on the link in a way that Gauss’s law, now including the dynamical charges, will hold in both the edges. In this staggered representation, even vertices represent “particles”, with a positive mass m , and odd ones - “holes”, with a negative mass $-m$. In fact, the negative vertices may be interpreted as the Dirac sea: suppose we shift the energy by a constant, and measure the mass of the odd vertices with respect to $-m$. Then an occupied odd vertex corresponds to a state with zero mass - no particle at all, and a vacant odd vertex corresponds to an anti-particle with mass m . This corresponds to the canonical transformation of second quantized Dirac fields, where the holes’ creation operators are replaced with anti-particles’ annihilation operators. We can also define the charges of the particles: the particle would have charge 1 (in units of the fundamental charge, of coupling constant g), and the anti-particle - charge -1. This means, in the language of fermionic operators, that

$$Q_n = \psi_n^\dagger \psi_n - \frac{1}{2} \left(1 - (-1)^{\sum_k n_k} \right) \quad (43)$$

and this completes the particle–anti-particle picture.

These two possible interactions may be understood as the meaning of *local gauge invariance*. Note that the only two possibilities of contracting gauge invariant operators are traces of products of group elements along closed loops, or along open loops, bounded by two fermionic operators on the edges. These two interactions are the shortest such interactions possible, and thus the most local ones. The same considerations apply as well to other lattice gauge theories.

* Note that staggered fermions are not the only possible recipe for discretization of fermionic fields, required by the doubling problem [159, 160, 90, 153, 154, 155, 156]. The different approaches, which are out of the scope of this paper, vary in both quantitative and qualitative details, and have their own advantages and disadvantages. Yet, when a quantum simulator is designed, one should consider which type of lattice fermions to use. We mostly use the staggered fermions formulation, but other approaches should be possible as well.

2.2.2. \mathbb{Z}_N . Another Abelian gauge theory of relevance is \mathbb{Z}_N . This is a *discrete* group, and thus this is not a Yang-Mills theory, and its structure is a little different. Nevertheless one can use this group to formulate a lattice gauge theory and observe interesting physics. This group is highly relevant for the confinement in *QCD*, as \mathbb{Z}_3 is the center of this group, and the center is responsible for confinement (large-distance phenomena) [161].

On every link of the lattice, we define two unitary operators, P and Q [162], such that

$$P^\dagger P = Q^\dagger Q = 1 \tag{44}$$

which satisfy the \mathbb{Z}_N algebra,

$$P^N = Q^N = 1 \quad ; \quad P^\dagger Q P = e^{i\delta} Q \tag{45}$$

where $\delta = \frac{2\pi}{N}$.

Let us define the eigenstates of P as

$$P |m\rangle = e^{im\delta} |m\rangle \tag{46}$$

there are N such states,

$$m \in \left\{ -\frac{N-1}{2}, \dots, \frac{N-1}{2} \right\} \tag{47}$$

for an odd N (the generalization for an even N is straightforward). Q is a unitary ladder operator,

$$Q |m\rangle = |m-1\rangle \tag{48}$$

with the cyclic property

$$Q \left| -\frac{N-1}{2} \right\rangle = \left| \frac{N-1}{2} \right\rangle \tag{49}$$

alternatively, one may use the eigenstates of Q , and then P will be a unitary raising operator, cyclic as well.

One can define Hermitian operators E, A such that

$$P = e^{i\delta E} \quad Q = e^{iA} \tag{50}$$

and in the $N \rightarrow \infty$ limit they will correspond to *cQED*'s conjugate electric field and vector potential.

The Hamiltonian of this theory takes the form [162]

$$H = -\frac{\lambda}{2} \sum_{\mathbf{n},k} \left(P_{\mathbf{n},k} + P_{\mathbf{n},k}^\dagger \right) - \frac{1}{2} \sum_{\text{plaq.}} \left(Q_1 Q_2 Q_3^\dagger Q_4^\dagger + H.c. \right) \tag{51}$$

with local terms and plaquette interactions, which tend to the Abelian Kogut-Susskind Hamiltonian (37) as $N \rightarrow \infty$. The plaquette indexing convention is, again, according to figure 3.

One can define static modular charges the vertices

$$q_{\mathbf{n}} = e^{-i\delta m} \tag{52}$$

and then the Gauss's law is given by

$$G_{\mathbf{n}} |\phi\rangle = q_{\mathbf{n}} |\phi\rangle \tag{53}$$

where

$$G_{\mathbf{n}} = \prod_{l_+} P_{l_+}^\dagger \prod_{l_-} P_{l_-} \quad (54)$$

with l_+ being links which start from \mathbf{n} (positive links) and l_- - ending there (negative ones).

A description of gauge theories with finite groups (both Abelian and non-Abelian), with dynamical, fermionic matter as well, is found in [163].

2.3. Non-Abelian Yang-Mills Theories: $SU(2)$ as an example

As an example of a continuous Non-Abelian gauge theory, we examine next the $SU(2)$ gauge theory [157, 90]. $SU(2)$ (the rotation group) has three generators, with the structure constants

$$f_{ijk} = \epsilon_{ijk} \quad (55)$$

which implies for the left and right algebras

$$\left[L_{\mathbf{n},k}^i, L_{\mathbf{n},k}^j \right] = -i\epsilon_{ijl} L_{\mathbf{n},k}^l \quad (56)$$

$$\left[R_{\mathbf{n},k}^i, R_{\mathbf{n},k}^j \right] = i\epsilon_{ijl} R_{\mathbf{n},k}^l \quad (57)$$

The pure-gauge Hamiltonian is (35). One may choose the representation of the U matrices, and let us do that in the fundamental representation of $SU(2)$ ($j = \frac{1}{2}$). In this representation we work with the Pauli matrices,

$$T^i = \frac{1}{2} \sigma^i \quad (58)$$

and thus

$$U_{\mathbf{n},k} = e^{\frac{i}{2} \theta_{\mathbf{n},k}^i \sigma^i} \quad (59)$$

- which are 2×2 matrices of operators. The reader may find an explicit expression for this operators, using the formulation [163], when we discuss the quantum simulation of this model.

The links' local Hilbert space, in the flux basis, is now described using three quantum numbers $|jmm'\rangle$. These are eigenstates of the operators

$$\mathbf{L}^2 |jmm'\rangle = \mathbf{R}^2 |jmm'\rangle = j(j+1) |jmm'\rangle \quad (60)$$

$$L_z |jmm'\rangle = m |jmm'\rangle \quad (61)$$

$$R_z |jmm'\rangle = m' |jmm'\rangle \quad (62)$$

A mechanical interpretation of this Hilbert space may be a rigid body, described in both body and space coordinates. In both of them the total angular momentum is equal, but in these two frames of reference the components of the angular momentum will be measured differently, as they form two separate, commuting algebras - the body and the space algebras, corresponding to the two algebras we have here [157, 164].

By acting with the group elements, which are rotation matrices, on the $|JMM'\rangle$ states, an amount of angular momentum is given to the state (or taken from it). Unlike in the $U(1)$ case, where the angular momentum is described by a single quantum number, here the representation is also a dynamical quantity: for example, acting with

$U_{\mathbf{n},k}$ in the fundamental representation on a $|JMM'\rangle$ state means adding a $\frac{1}{2}$ quanta of angular momentum to the state, resulting in a superposition of $J + \frac{1}{2}$ and $J - \frac{1}{2}$ states (ordinary addition of angular momentum). Quantitatively this is expressed by [165]

$$U_{mm'}|JMM'\rangle = C_+ \left| J + \frac{1}{2}, M + m, M' + m' \right\rangle + C_- \left| J - \frac{1}{2}, M + m, M' + m' \right\rangle \quad (63)$$

where C_{\pm} depend on the appropriate Clebsch-Gordan coefficients [165, 166]. Thus the representation of the state, the quantum number J , is a dynamical observable here, unlike in continuum field theories, where each field has a constant, well-defined, static representation: this is due to the fact that lattice gauge fields are not Fock-space bosons [163].

If one wishes to include dynamical fermions as well, the interaction with which shall be described by a Hamiltonian of the form (9), where $\psi_{\mathbf{n}}$ are *group spinors*. Thus, if we pick U to be in the fundamental representation, this will also be the case for the spinors, which will contain now two components - each Lorentz component will be such a spinor. With staggered fermions we shall have such a single color spinor on each vertex. In this case the charges will simply be [157, 90]

$$Q_{\mathbf{n}}^a = \frac{1}{2} \sum_{ij} \psi_{\mathbf{n},i}^{\dagger} (\sigma^a)_{i,j} \psi_{\mathbf{n},j} \quad (64)$$

satisfying the group's algebra. Note that the ‘‘Dirac sea’’ state can be obtained here as well (as a no-interactions vacuum). Again, we measure the mass of each particle with respect to $-m$, and a fully occupied vertex, due to the fermionic nature of the matter particles, corresponds to zero charge. Thus the Dirac sea is the case with empty even vertices and fully occupied (by two fermions) odd vertices [167].

The description of other $SU(N)$ groups is similar; Changing the group means changing the local Hilbert spaces, but the Hamiltonian has the same form. A description of Hamiltonian lattice compact QCD ($SU(3)$) is given in [100].

2.4. Physical content of the models

Gauge theories in general, including ones on the lattice, exhibit an interesting phase structure. These include, for example, QCD 's phases of color-superconductivity or quark-gluon plasma [94, 100, 101], whose treatment using the usual Monte-Carlo methods utilized in lattice gauge theory is rather problematic, due to the computationally hard sign problem [99] that limits calculations in regimes with a finite chemical potential for the fermions.

Another interesting and important property of gauge theories is the existence of confining phases, dependent on the coupling constant and other parameters. We shall review quark confinement in pure gauge theories in detail below.

2.4.1. Quark Confinement. Free quarks are not found in nature, but rather bind together and form hadrons, such as baryons and mesons. The reason to that is the physical phenomenon of quark confinement, manifested in QCD but also in other gauge theories: in large distances, or low energies, the static potential between quarks is linear in the distance, and thus it is energetically unfavorable (and practically impractical) to separate bound quarks. It is a highly intriguing concept, forming

a fundamental aspect in the understanding of the Hadronic spectrum, involving nontrivial low energy physics, which cannot be addressed perturbatively.

Schwinger showed, by exactly solving 1+1 dimensional QED with massless charges [102, 103], that vector mesons can be massive if massless fermions are screened by the vacuum polarization, obtaining massive photons. Further studies [104, 105] have shown that only massive photons, no electrons, exist in the asymptotic states of this model. The latter work has also shown, in accordance with the expected confining behavior, that electrons arise in deep-inelastic-scattering scenarios - i.e., short distances and high energies, and they behave like free pointlike particles (agreeing with the “parton model”, or the asymptotic freedom of QCD , where the confined quarks are asymptotically free within the hadrons - at short ranges and high energies). The existence of massive photons is in accordance with the fact that in terms of statistical mechanics, confinement is a gapped, disordered phase, while the ordered phases do not confine [168, 158].

A significant step in the study of confinement was done by Wilson, who introduced lattice gauge theory for this purpose [88]. Using loops in lattice gauge theory, which were later called “Wilson Loops”, he showed that 3+1 dimensional compact QED has a confining phase (for strong coupling, $g^2 \gg 1$), which binds charges together and forbids the existence of free electrons and positrons, as well as a Coulomb phase (for weak coupling, $g^2 \ll 1$), as in continuous QED . It was shown later (see subsection 2.4.3) that 2+1 dimensional $cQED$ confines for all values of the coupling constant [106]: confinement in compact QED was identified as a topological effect, having to do with instantons and magnetic monopoles. This result was supported by other works as well [107, 108, 109].

Similarly to the “charge confinement” in Abelian theories, confinement also takes place in non-Abelian gauge theories, such as non-Abelian Yang-Mills theories (as QCD) as well as the discrete theory of \mathbb{Z}_N presented earlier. It was argued [161] that large-distance phenomena, involving the confinement of quarks in QCD , is related with the group’s center - \mathbb{Z}_3 , which makes the phase structure of \mathbb{Z}_N interesting [162, 169, 170]: The theory confines in the strong coupling limit ($\lambda \rightarrow \infty$). In 2+1 and 3+1 dimensions it is not the only phase. In 3 + 1 dimensions, due to the self-duality of the \mathbb{Z}_N theory, there is a phase transition from electric confinement (strong coupling) to magnetic confinement (weak coupling), for $N < N_c$ ($N_c \sim 6$). For $N > N_c$ there is a third phase, with no confinement at all. In 2+1 dimensions there is a phase transition to a non-confining phase in the weak limit [168, 162]. However, for $N \rightarrow \infty$ the theory shows the phase transition at $g = 0$ [170], in accordance with the single confining phase structure of $U(1)$ (the $N \rightarrow \infty$ limit of \mathbb{Z}_N).

Both in $U(1)$ and $SU(N)$, one can show, using perturbation theory, the confinement of charges/quarks in the strong coupling limit, as will be done in subsection 2.4.2. The confinement of static charges is manifested by “electric flux tubes” connecting them, which get thicker as the coupling constant decreases. But, outside the strong limit, confinement (in cases it holds) becomes nontrivial and requires nonperturbative techniques, and for Yang-Mills theories it is still an open question: in fact, the proof and calculation of the Mass Gap in Yang-Mills theories, which is related to quark confinement, is one of Clay’s institute Millennium Prize problems. For example, in the cases confinement was proven, it was mostly done for static charges - and not dynamical fermions.

Dynamical fermions shall enhance electric flux-tube breaking. If one stretches a flux tube, at a certain point it would be energetically favorable to create two pair of

“new” quarks, or charges, breaking the a long flux tube into two smaller ones.

2.4.2. Strong Coupling Lattice Gauge Theories. An interesting limit of lattice Yang-Mills theories is the strong coupling limit $g^2 \gg 1$, in which the Kogut-Susskind Hamiltonian (35) may be treated perturbatively: the magnetic, plaquette part H_B may be treated as a perturbation to the electric $H_E \equiv H_0$. ‡

Consider two opposite static charges, placed on the vertices \mathbf{n} and $\mathbf{n} + R\hat{\mathbf{x}}$ of a lattice. What is the ground state of this static charge configuration in the strong coupling limit? In this limit, products of local (links) electric field states form a good basis, as they are eigenstates of H_E , and thus we obviously must find the electric field configuration with minimal energy, which satisfies the *static* Gauss’s law for these two charges.

The no-charge vacuum of this limit satisfies

$$|\Omega (g^2 \gg 1)\rangle = \otimes_{\mathbf{n},k} |0\rangle \quad (65)$$

- on each link the state satisfies

$$\mathbf{L}^2 |0\rangle = 0 \quad (66)$$

- no electric field at all.

If we excite a link (using U) the zeroth order energy is increased by a unit of \mathbf{L}^2 :

$$\mathbf{L}^2 U |0\rangle = [\mathbf{L}^2, U] |0\rangle = \left(\sum_a T_i^{(r)} T_i^{(r)} \right) U |0\rangle \quad (67)$$

where T_i^r is the matrix representation of the group’s generator in representation r , and $C_2(r) \equiv \sum_i T_i T_i$ is just a C-number - the eigenvalue of the Casimir operator in this representation.

Thus, for example, in the case of *cQED*, we get [89]

$$L^2 U |0\rangle = U |0\rangle \quad (68)$$

and in the case of *SU(2)*, for charges in the fundamental representation $j = \frac{1}{2}$ [90],

$$\mathbf{L}^2 U |0\rangle = \left(\frac{1}{4} \sum_a \sigma_a \sigma_a \right) U |0\rangle = \frac{3}{4} U |0\rangle \quad (69)$$

or in any other representation r ,

$$\mathbf{L}^2 U^r |0\rangle = j_r (j_r + 1) U^r |0\rangle \quad (70)$$

This means that if we have N links with a single excitation, the energy of the state (in zeroth order) will be $\frac{Ng^2}{2} C_2(r)$. In order to respect Gauss’s law (and fulfill gauge invariance), the eigenstates of H_E in this charge configuration will contain a

‡ It is worth to comment that strong coupling calculations were initially performed in the Euclidean formalism. The first to do that was Wilson [88].

flux line of $U|0\rangle$ states, ranging between the charges. The minimal energy is obtained for the direct line, and thus the ground state is:

$$|R_{0,mm'}\rangle = \left(\prod_{\mathbf{n}=\mathbf{n}}^{\mathbf{n}+(R-1)\hat{\mathbf{x}}} U_{\mathbf{n},x} \right)_{mm'} |\Omega\rangle \quad (71)$$

††. This flux-line is the so-called *electric flux tube*, manifesting confinement. The zeroth order energy of this state is

$$E_0 |R_{0,mm'}\rangle = H_E |R_{0,mm'}\rangle = \frac{g^2}{2} C_2(r) R |R_{0,mm'}\rangle \quad (72)$$

and thus we get that the strong coupling limit confines, with a *string tension* (the ratio between the static potential and the distance) of

$$\sigma_{strong} = \frac{g^2}{2} C_2(r) \quad (73)$$

Such a flux-tube connecting the appropriate pair of them is nothing but a *meson*. One could also create a long flux tube connecting static charges and watch it dynamically breaking into shorter, energy favorable tubes, by dynamic pair creation. Also, as mentioned before, outside the strong limit, but within the confining phase, the state shall be modified such that the flux-tube is thicker (wider than just a thin, single lattice line).

2.4.3. The Weak Limit of cQED . As g decreases, perturbative corrections must be taken into account, until perturbation theory breaks down and nonperturbative methods of the weak regime must be utilized. As an example, we shall comment about the weak limit of *cQED*.

In 3+1 dimensions, one can use continuum limit Wilson loop arguments [89], as the weak limit corresponds to the continuum limit, and obtain the Coulomb potential.

In 1+1 dimensions, on the other hand, the theory confines for all values of the coupling constant, as it is solvable and has no dependence on the coupling constant g . This was shown (for the massless case) in the continuum by Schwinger [102, 103], but similar results apply also in the lattice compact case in [171] (as well as in other, more recent, lattice studies, such as using tensor network states [172, 173, 174, 175, 176, 177, 178]).

In 2+1 dimensions interesting physics takes place, involving instantons and topological effects. Due to magnetic monopoles, there is a mass gap in the weak limit, corresponding to quark confinement. This was shown by Polyakov [106] using Euclidean partition functions, by Drell, Quinn, Svetitsky and Weinstein, [108] using variational Hamiltonian approach, and by Banks, Myerson and Kogut [107], using the Villain approximation. The three approaches were compared by Ben-Menahem [109] who also demonstrated that compactness is necessary for confinement in lattice *QED*.

††The indices in the state are another manifestation of the fact we disregard the charge degrees of freedom in this context. If one introduces the matter operators $\psi_{\mathbf{n}}$, the operator creating the state out of the full vacuum would be $\sum_{mm'} \psi_{\mathbf{n},m}^\dagger \left(\prod_{\mathbf{n}=\mathbf{n}}^{\mathbf{n}+(R-1)\hat{\mathbf{x}}} U_{\mathbf{n},x} \right)_{mm'} \psi_{\mathbf{n}+\mathbf{R}\hat{\mathbf{x}},m'} = \psi_{\mathbf{n}}^\dagger \prod_{\mathbf{n}=\mathbf{n}}^{\mathbf{n}+(R-1)\hat{\mathbf{x}}} U_{\mathbf{n},x} \psi_{\mathbf{n}+\mathbf{R}\hat{\mathbf{x}}}$ which we easily identify as a gauge invariant string.

In some sense, the confinement mechanism of 2+1 dimensional $cQED$ is more related to the confinement of quarks in QCD , as both of them are topological effects.

The discussion above applies for zero temperature. For a finite, nonzero temperature, a Coulomb phase arises for weak values of the coupling constant, with a phase transition to the Coulomb phase at some value of T, g [93, 95].

3. Ultracold Atoms in Optical Lattices : A brief review

3.1. Generation of an Optical Potential

Optical lattices are created by “external”, classical lasers, and virtual processes to an excited atomic state [7, 26, 9, 11].

Consider a two level atom (disregard the other levels), whose levels are $|\alpha\rangle$ - some meta-stable level (in which the atom is initially prepared), and $|e\rangle$ - an excited one (see figure 4). We may write its Hamiltonian in the form

$$H_{atom} = \frac{\mathbf{p}^2}{2m} + \omega_e |e\rangle \langle e| \quad (74)$$

The atoms are usually alkaline, therefore they have a single valence electron, which simplifies their treatment by many aspects.

The atom experiences an external, classical laser field, of the form

$$\mathbf{E}(\mathbf{x}, t) = E(\mathbf{x}) e^{-i\omega t} \hat{\epsilon} \quad (75)$$

Switching to a system rotating with the laser’s frequency ω , and defining the detuning $\delta = \omega_e - \omega$ (see figure 4), we get

$$H_{atom} = \frac{\mathbf{p}^2}{2m} + \delta |e\rangle \langle e| \quad (76)$$

The interaction between the laser and the atom is given in the dipole approximation, which is valid if we assume that the electric field’s amplitude varies slowly compared to the atomic size (in space) and $1/\omega$ (in time; Note that here, for simplicity, the amplitude was not even considered as having a time dependence, but one may generalize to a time-dependent amplitude, of the form $E(\mathbf{x}, t)$). This interaction has the form

$$H_{dipole} = -\mathbf{d} \cdot \mathbf{E}(\mathbf{x}, t) \quad (77)$$

where \mathbf{d} is the dipole moment of the operator; After transforming to the rotating frame, performing a rotating wave approximation (neglecting the fast-rotating terms) and plugging $d_{ij} = \hat{\epsilon} \cdot \langle i | \mathbf{d} | j \rangle$, the dipole moment matrix elements (projected on the laser’s polarization), one obtains the interaction Hamiltonian

$$H_{dipole} = -d_{e\alpha} E(\mathbf{x}) |e\rangle \langle \alpha| + h.c. \equiv \frac{\Omega(\mathbf{x})}{2} |e\rangle \langle \alpha| + h.c. \quad (78)$$

where

$$\Omega(\mathbf{x}) = -2E(x) d_{e\alpha} \quad (79)$$

is the Rabi frequency ($d_{e\alpha} = d_{\alpha e}$, as the dipole operator is Hermitian).

We assume that the detuning δ is sufficiently large - the coupling is non-resonant, and that transitions between the atomic levels are practically impossible. However,

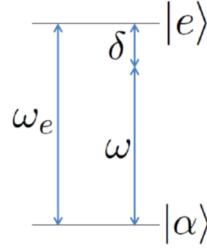


Figure 4. The energy levels of the trapped atom. $|\alpha\rangle$ is the meta-stable level, for which the optical potential is effectively obtained by eliminating the excited level $|e\rangle$. The levels are separated by frequency ω_e , and they are coupled non-resonantly with a laser of frequency ω : the detuning is $\delta = \omega_e - \omega$.

virtual second-order transitions to the excited level and back are possible, and thus we get the effective Hamiltonian (for the $|\alpha\rangle$ subspace)

$$H = \frac{\mathbf{p}^2}{2m} + V_{op}(\mathbf{x}) \quad (80)$$

where

$$V_{op}(\mathbf{x}) = -\frac{|\Omega(\mathbf{x})|^2}{4\delta} \quad (81)$$

is called the optical trapping potential, and it is an effective potential experienced by the atom in the $|\alpha\rangle$ state. In fact, this is merely the AC Stark effect. Note that we have actually “traced out” the internal levels, due to the energy restriction (large detuning) and what we now have is a configuration space Hamiltonian. Choosing the effective field properly, one could generate an optical lattice: a periodic trapping potential, allowing the trapped atoms to fill its minima. Since $V_{op}(\mathbf{x}) \propto |E(\mathbf{x})|^2$, a standing wave of the form $E(x) = E_0 \cos(kx)$ would result, for example, in an optical potential of the form $V_{op}(x) = V_0 \cos^2(kx)$; One could add lasers in more than one direction to obtain a two- and three-dimensional optical lattices of various geometries.

Next we shall consider an optical lattice with many atoms. This shall be done in the context of second quantization, for which we are interested in the single-particle eigenfunctions of the trapping Hamiltonian.

Due to the lattice symmetry, the single particle wavefunctions are merely Bloch waves. These states are not localized, therefore if one wishes to work in the number basis of local minima (Fock basis), a transformation to local single particle wavefunctions is required. This is fulfilled by the orthonormal basis of Wannier functions, $w_n(\mathbf{x} - \mathbf{x}_0)$, which are the discrete Fourier transform of the Bloch wavefunctions $u_{\mathbf{q}}^{(n)}(\mathbf{x})$ over the lattice [26, 9, 11]:

$$w_n(\mathbf{x} - \mathbf{x}_0) \propto \sum_{\mathbf{q}} e^{-i\mathbf{q} \cdot \mathbf{x}_0} u_{\mathbf{q}}^{(n)}(\mathbf{x}) \quad (82)$$

These states are labeled by n , which is the energy band, and are each spatially centered around a different local minimum \mathbf{x}_0 of the optical potential. These are the desired local site (minimum) wavefunctions.

Working in low enough temperatures, it is reasonable to include only the lowest energy band, $w_0(\mathbf{x} - \mathbf{x}_0)$.

One can expand the second-quantization “wavefunction” of the condensates in terms of the localized Wannier functions $\phi_{\mathbf{n}}(\mathbf{x}) \equiv w_0(\mathbf{x} - \mathbf{x}_{\mathbf{n}})$ and single particle annihilation operators $a_{\mathbf{n}}$ (bosonic or fermionic, depending on the statistics of the atoms), both defined at the site (minimum of the potential) \mathbf{n} , as

$$\Phi(\mathbf{x}) = \sum_{\mathbf{n}} a_{\mathbf{n}} \phi_{\mathbf{n}}(\mathbf{x}) \quad (83)$$

and construct from which a usual second quantization Hamiltonian density:

$$\mathcal{H} = \Phi^\dagger(\mathbf{x}) \left(-\frac{\nabla^2}{2m} + V_{op}(\mathbf{x}) + V_T(\mathbf{x}) \right) \Phi(\mathbf{x}) + \int d^3x' \int d^3x \Phi^\dagger(\mathbf{x}') \Phi^\dagger(\mathbf{x}) V(\mathbf{x} - \mathbf{x}') \Phi(\mathbf{x}) \Phi(\mathbf{x}') \quad (84)$$

where $V_T(\mathbf{x})$ is an external trapping potential, varying slowly compared to the optical lattice potential $V_{op}(\mathbf{x})$, and $V(\mathbf{x} - \mathbf{x}')$ is some two-body interaction, which will be specified later.

3.2. Multi-species Lattices and Spinor Condensates

It is also possible to utilize more atomic levels and transitions and create a “species-dependent lattice”: i.e., with different minima for different atomic species, which may be, for example, different atomic hyperfine levels [179, 180, 26, 8, 11].

The atomic hyperfine structure is given by an $SU(2)$ Hilbert space, characterized by two quantum numbers F, m_F . Just like “regular” angular momentum,

$$\mathbf{F}^2 |F, m_F\rangle = F(F+1) |F, m_F\rangle \quad (85)$$

and

$$F_z |F, m_F\rangle = m_F |F, m_F\rangle \quad (86)$$

\mathbf{F} is defined as

$$\mathbf{F} = \mathbf{I} + \mathbf{L} + \mathbf{S} \quad (87)$$

where \mathbf{I} is the nuclear spin, and \mathbf{L}, \mathbf{S} stand for the valence electron’s orbital angular momentum and spin respectively (recall that we are dealing with alkaline atoms, with a single valence electron), and thus the Lie algebra

$$[F_i, F_j] = i\epsilon_{ijk} F_k \quad (88)$$

is satisfied. Each species $|\alpha\rangle$ can then experience a different optical potential $V_{op}^\alpha(\mathbf{x})$, and these potentials form a *superlattice*.

Such lattices / condensates are sometimes referred to as spinor lattices / condensates.

As an example, consider ^{87}Rb and ^{23}Na have a nuclear spin $I = \frac{3}{2}$. Thus, in the S-wave hyperfine manifold (which is relevant for ultracold atoms, as explained in subsection 3.3), $F = 1$ or 2 .

We denote the internal levels by Greek indices, and the second-quantization expansion generalizes to

$$\Phi_\alpha(\mathbf{x}) = \sum_{\mathbf{n}} a_{\mathbf{n},\alpha} \phi_{\mathbf{n},\alpha}(\mathbf{x}) \quad (89)$$

for each species, where the Wannier functions may be species dependent or independent - depending on the lattice structure and symmetry and the choice of these levels.

The Hamiltonian density is now

$$\begin{aligned} \mathcal{H} = & \sum_{\alpha,\beta} \Phi_{\alpha}^{\dagger}(\mathbf{x}) \left(\delta^{\alpha\beta} \left(-\frac{\nabla^2}{2m} + V_{op}^{\alpha}(\mathbf{x}) + V_T(\mathbf{x}) \right) + \Omega^{\alpha\beta}(\mathbf{x}) \right) \Phi_{\beta}(\mathbf{x}) \\ & + \sum_{\alpha,\beta,\gamma,\delta} \int d^3x' \Phi_{\alpha}^{\dagger}(\mathbf{x}') \Phi_{\beta}^{\dagger}(\mathbf{x}) V_{\alpha\beta\gamma\delta}(\mathbf{x} - \mathbf{x}') \Phi_{\gamma}(\mathbf{x}) \Phi_{\delta}(\mathbf{x}') \end{aligned} \quad (90)$$

where $\Omega^{\alpha\beta}(\mathbf{x})$ corresponds to a Rabi coupling of atomic levels by more lasers.

3.3. Scattering of Ultracold Atoms

How cold is ultracold? The ultracold regime is defined as the one in which the lowest partial wave governs the scattering. It is a dilute and cold regime.

We are dealing with the so called *weak interaction regime*, involving the ground state of a gas of either bosonic or fermionic atoms. For ideal bosons, we assume that they all occupy the lowest energy band (Bose Einstein Condensate). A phase transition from Bose-Einstein condensate takes place in a finite temperature (in three dimensions), when the thermal de-Broglie wavelength $\lambda_T = \sqrt{\frac{2\pi}{k_B T}}$ (in $\hbar = 1$ units) approaches $n^{-1/3}$ - the average inter-particle distance (n is the number density). For fermions, the states are full up to the Fermi energy, ϵ_F : for temperatures satisfying $k_B T \ll \epsilon_F$ the gas is considered degenerate [9].

When the energy is low enough - i.e., the de-Broglie wavelength of the atoms is much larger than the effective range of the potential [11], the interaction potential in (84) is accurately described by the pseudopotential:

$$V(\mathbf{x} - \mathbf{x}') = \frac{2\pi a}{m} \delta^{(3)}(\mathbf{x} - \mathbf{x}') \equiv \frac{g}{2} \delta^{(3)}(\mathbf{x} - \mathbf{x}') \quad (91)$$

For bosons the scattering is governed by the S-wave channel. For identical fermions, on the other hand, due to Pauli's exclusion principle, there is no S-wave scattering [9]; This is not a problem for the scattering of two different fermions (non-identical).

The density of the atoms, n , is typically $10^{12} - 10^{15} \text{cm}^{-3}$. This gives a typical interparticle distance $n^{-1/3}$ of the order of $0.1 - 10 \mu\text{m}$, and the scattering length is in the range of few nanometers [9]. The scattering length of ^{87}Rb , for example, has on order of magnitude of 100 times the Bohr radius, varying slightly according to the different internal states [180]. The gas is sufficiently dilute for $n^{1/3}a \ll 1$, in case of bosonic repulsive interactions ($a > 0$), as $\sqrt{na^3}$ is the small parameter of the Bogolyubov theory, describing weakly interacting Bose gases [9].

We thus obtain a simplified version for the single-species case Hamiltonian density:

$$\mathcal{H} = \Phi^{\dagger}(\mathbf{x}) \left(-\frac{\nabla^2}{2m} + V_{op}(\mathbf{x}) + V_T(\mathbf{x}) \right) \Phi(\mathbf{x}) + \frac{g}{2} \Phi^{\dagger}(\mathbf{x}) \Phi^{\dagger}(\mathbf{x}) \Phi(\mathbf{x}) \Phi(\mathbf{x}) \quad (92)$$

after plugging in the Wannier functions and creation/annihilation operators (83) one may integrate over the Wannier functions. Using the overlap integrals

$$\epsilon_n = \int d^3x \phi_n^*(\mathbf{x}) \left(-\frac{\nabla^2}{2m} + V_{op}(\mathbf{x}) + V_T(\mathbf{x}) \right) \phi_n(\mathbf{x}) \quad (93)$$

$$J_{mn} = \int d^3x \phi_m^*(\mathbf{x}) \left(-\frac{\nabla^2}{2m} + V_{op}(\mathbf{x}) + V_T(\mathbf{x}) \right) \phi_n(\mathbf{x}) \quad (94)$$

$$U_{mnl} = g \int d^3x \phi_m^*(\mathbf{x}) \phi_n^*(\mathbf{x}) \phi_k(\mathbf{x}) \phi_l(\mathbf{x}) \quad (95)$$

where m, n, k, l label the lattice sites. The most general Hamiltonian, taking into account all possible overlap integrals, is

$$H = \sum_{m,n} J_{m,n} a_m^\dagger a_n + \sum_{m,n,k,l} U_{m,n,k,l} a_m^\dagger a_n^\dagger a_k a_l \quad (96)$$

3.4. Multiple Species Scattering

In case of multiple species, the most general form of the Hamiltonian is

$$H = \sum_{m,n,\alpha,\beta} J_{m,n}^{\alpha,\beta} a_{m,\alpha}^\dagger a_{n,\beta} + \sum_{m,n,k,l,\alpha,\beta,\gamma,\delta} U_{m,n,k,l}^{\alpha,\beta,\gamma,\delta} a_{m,\alpha}^\dagger a_{n,\beta}^\dagger a_{k,\gamma} a_{l,\delta} \quad (97)$$

however, if we remember that the species are different hyperfine states, and take into account the hyperfine rotational symmetry (conservation of the hyperfine angular momentum in atomic collisions) we can simplify this Hamiltonian further, as we shall do next [179, 180].

Suppose we wish to consider the scattering of two atoms with distinct F, m_F values: for example, let us scatter an F_1 atom on an F_2 atom. As a result, we shall get a pair of two atoms with their own F, m_F values. However, taking into account the rules of addition of angular momenta, one should be aware that the scattering may take place “through” an “intermediate state” with several values of total angular momentum F_T . Thus, the effective scattering potential will take the form

$$V_{\alpha,\beta,\gamma,\delta}(\mathbf{x} - \mathbf{x}') = \frac{2\pi}{m} \delta^{(3)}(\mathbf{x} - \mathbf{x}') \sum_{F_T} a_{F_T} (P_{F_T})_{\alpha,\beta,\gamma,\delta} \quad (98)$$

where we sum over the possible values of total angular momentum F_T , and consider, for each value, its corresponding scattering length a_{F_T} . P_{F_T} is the projection operator onto the subspace of total angular momentum F_T . In case of different atomic masses, the appropriate reduced masses should replace the mass m .

The projection operators can be represented using functions of $\mathbf{F}_1 \cdot \mathbf{F}_2$. Physically, that may be understood as a consequence of rotational invariance: terms which depend on the F values of two atoms and conserve the hyperfine angular momentum must be constructed out of powers of these terms. Mathematically,

$$\mathbf{F}_1 \cdot \mathbf{F}_2 = \frac{1}{2} (\mathbf{F}_T^2 - \mathbf{F}_1^2 - \mathbf{F}_2^2) \quad (99)$$

and as $\mathbf{F}_1^2, \mathbf{F}_2^2$ are practically constants for our purposes, a function of $\mathbf{F}_1 \cdot \mathbf{F}_2$ is in fact a function of \mathbf{F}_T^2 , and thus one can construct the projection operators out of this scalar product. If there are n possible values of total hyperfine angular momentum, the projection operators are polynomials of the form

$$P_{F_T} = \sum_{k=0}^{n-1} G_{F_T,k} (\mathbf{F}_1 \cdot \mathbf{F}_2)^k \quad (100)$$

and eventually obtain

$$V_{\alpha,\beta,\gamma,\delta}(\mathbf{x} - \mathbf{x}') = \delta^{(3)}(\mathbf{x} - \mathbf{x}') \frac{g_k}{2} \left((\mathbf{F}_1 \cdot \mathbf{F}_2)^k \right)_{\alpha,\beta,\gamma,\delta} \quad (101)$$

where the $\{g_k\}$ coefficients depend simply on the scattering lengths $\{a_{F_T}\}$ and the coefficients in the projection operators' expansion, $\{G_{F_T,k}\}$, involved. The scattering lengths are tunable using Feshbach resonances, either magnetic or optical [181, 182, 183, 184, 185, 186, 180, 9, 187, 188].

We can also express the projection operators, and thus the scattering potential, in terms of the Clebsch-Gordan coefficients:

$$V_{\alpha,\beta,\gamma,\delta}(\mathbf{x} - \mathbf{x}') = \delta^{(3)}(\mathbf{x} - \mathbf{x}') \sum_{F_T} C_{F_T} \langle F_1, m_{F_1} = \alpha; F_2, m_{F_2} = \beta | F_T, M_F \rangle \times \\ \langle F_T, M_F | F_1, m_{F_1} = \gamma; F_2, m_{F_2} = \delta \rangle$$

which explicitly manifests, as a consequence of hyperfine angular momentum conservation, that $\alpha + \beta = \gamma + \delta$, and the $\{C_{F_T}\}$ coefficients depend on the scattering lengths.

As an example [179, 180], one may consider a spinor condensate of $F = 1$. The possible values of total angular momentum in collisions are naively $F_T = 0, 1, 2$, but since the atoms are bosons, and the states must be symmetric, we remain with $F_T = 0, 2$. Thus the scattering lengths we need are a_0 and a_2 , and the highest power of $\mathbf{F}_1 \cdot \mathbf{F}_2$ we need is 1. The projection operators are

$$P_0 = \frac{1}{3} (1 - \mathbf{F}_1 \cdot \mathbf{F}_2) \quad (102)$$

and

$$P_2 = \frac{1}{3} (\mathbf{F}_1 \cdot \mathbf{F}_2 + 2) \quad (103)$$

One can define

$$g_0 = \frac{4\pi}{3m} (2a_2 + a_0) \quad (104)$$

and

$$g_2 = \frac{4\pi}{3m} (a_2 - a_0) \quad (105)$$

and obtain the scattering part of the Hamiltonian density

$$\frac{g_0}{2} \sum_{\alpha,\beta} \Phi_\alpha^\dagger(\mathbf{x}) \Phi_\beta^\dagger(\mathbf{x}) \Phi_\beta(\mathbf{x}) \Phi_\alpha(\mathbf{x}) + \frac{g_2}{2} \sum_{\alpha,\beta,\gamma,\delta} (\Phi_\alpha^\dagger(\mathbf{x}) \mathbf{F}_{\alpha\gamma} \Phi_\gamma(\mathbf{x})) \cdot (\Phi_\beta^\dagger(\mathbf{x}) \mathbf{F}_{\beta\delta} \Phi_\delta(\mathbf{x})) \quad (106)$$

where \mathbf{F} are the $F = 1$ representation matrices of $SU(2)$.

3.5. Summary of the Available Interactions and Possibilities

To conclude, in optical lattices one could use either bosonic or fermionic ultracold atoms, of species $\{\alpha\}$, with single particle local wavefunctions at sites n , $\phi_{n,\alpha}(\mathbf{x})$ and $\psi_{n,\alpha}(\mathbf{x})$ for bosons and fermions respectively, and annihilation operators $a_{n,\alpha}$ and $c_{n,\alpha}$ for bosons and fermions respectively, satisfying the canonical commutation relations

$$[a_{n,\alpha}, a_{m,\beta}^\dagger] = \delta_{nm} \delta_{\alpha\beta} \quad (107)$$

$$\{c_{n,\alpha}, c_{m,\beta}^\dagger\} = \delta_{nm} \delta_{\alpha\beta} \quad (108)$$

$$[a_{n,\alpha}, a_{m,\beta}] = \{c_{n,\alpha}, c_{m,\beta}\} = [a_{n,\alpha}, c_{m,\beta}] = 0 \quad (109)$$

Out of these operators and wavefunctions, the second-quantization field operators are constructed,

$$\Phi_\alpha(\mathbf{x}) = \sum_n a_{n,\alpha} \phi_{n,\alpha}(\mathbf{x}) \quad (110)$$

$$\Psi_\alpha(\mathbf{x}) = \sum_n c_{n,\alpha} \psi_{n,\alpha}(\mathbf{x}) \quad (111)$$

and they are the ingredients of the atomic Hamiltonian, consisting of three main parts:

- (i) The single-particle terms,

$$H_0 = \sum_\alpha \int d^3\mathbf{x} (\Psi_\alpha^\dagger(\mathbf{x}) H_{0,f} \Psi_\alpha(\mathbf{x}) + \Phi_\alpha^\dagger(\mathbf{x}) H_{0,b} \Phi_\alpha(\mathbf{x})) \quad (112)$$

where $H_{0,f}, H_{0,b}$ are the fermionic and bosonic single-particle Hamiltonians, including the kinetic energy and the optical and trapping potentials. They depend on (or, from another perspective, affect) the shape of the lattice (through the optical potential) and thus the single-particle wavefunctions, $\phi_{n,\alpha}(\mathbf{x})$ and $\psi_{n,\alpha}(\mathbf{x})$.

- (ii) The scattering terms,

$$\begin{aligned} H_{sc} = & \frac{1}{2} \sum_{\alpha,\beta,\gamma,\delta} g_{\alpha\beta\gamma\delta}^{FF} \int d^3\mathbf{x} \Psi_\alpha^\dagger(\mathbf{x}) \Psi_\beta^\dagger(\mathbf{x}) \Psi_\gamma(\mathbf{x}) \Psi_\delta(\mathbf{x}) \quad (113) \\ & + \frac{1}{2} \sum_{\alpha,\beta,\gamma,\delta} g_{\alpha\beta\gamma\delta}^{BB} \int d^3\mathbf{x} \phi_\alpha^\dagger(\mathbf{x}) \phi_\beta^\dagger(\mathbf{x}) \phi_\gamma(\mathbf{x}) \phi_\delta(\mathbf{x}) \\ & + \frac{1}{2} \sum_{\alpha,\beta,\gamma,\delta} g_{\alpha\beta\gamma\delta}^{BF} \int d^3\mathbf{x} \Psi_\alpha^\dagger(\mathbf{x}) \phi_\beta^\dagger(\mathbf{x}) \Psi_\gamma(\mathbf{x}) \phi_\delta(\mathbf{x}) \end{aligned}$$

which govern the two-body S-wave scattering (atomic collisions), and depend on the scattering coefficients g . They depend on the scattering lengths, and of course on the nature of collisions - fermion-fermion (FF), boson-boson (BB) or boson-fermion (BF), and the atomic species involved. These coefficients are not independent of each other, thanks to the conservation of hyperfine angular momentum, and are tunable using Feshbach resonances.

- (iii) Rabi (laser) terms,

$$\begin{aligned} H_R = & \sum_{\alpha,\beta} \Omega_{\alpha\beta}^F \int d^3\mathbf{x} \Psi_\alpha^\dagger(\mathbf{x}) \Psi_\beta(\mathbf{x}) \\ & + \sum_{\alpha,\beta} \Omega_{\alpha\beta}^B \int d^3\mathbf{x} \phi_\alpha^\dagger(\mathbf{x}) \phi_\beta(\mathbf{x}) \end{aligned} \quad (114)$$

which are governed by external lasers and may induce desired hopping processes.

One could also include transitions to and from molecular states, but these are not of relevance for this report.

Current experimental technologies allow creating complex and controllable optical lattices. The range of parameters is wide, as exemplified by the typical numbers presented above: the ratio V_0/E_R is tunable. Optical lattices may be created in various geometries and dimensionalities, using holographic techniques, for example.

The lattices may be very large (for example, 150000 lattice sites in [20]) and contain many atoms. The atoms may be distributed across the lattice in various ways: lattice sites may occupy few atoms, even single ones [20, 189, 190, 30, 191], or much more (for example, 80 in [192], using tube-shaped sites).

Common measurements are the so-called “time-of-flight” measurements, in which the lattice is switched off (suddenly or adiabatically) and the atoms are released, in a way that their spatial density is proportional to their momentum distribution, which is measurable using standard imaging methods [9]. Contemporary experiments also demonstrate with great success single-addressability of lattice sites and atoms [192, 189, 190, 191], which opens the way for various possibilities, both in measurements and initial state preparation.

Further detailed information on the topic may be found in [11].

4. A framework for Quantum Simulation of lattice gauge theories with ultracold atoms in optical lattices

We shall review several methods for quantum simulation - i.e., physical realization using ultracold atoms in optical lattices, of three different lattice gauge theories: compact QED , $SU(N)$ and \mathbb{Z}_N .

In order to simulate a gauge theory, three requirements must be fulfilled [121]:

- (i) *The theory must contain both fermions and bosons.* The fermions will represent matter fields and the bosons - gauge fields. This makes ultracold atoms natural candidates, as bosonic and fermionic atoms are practically free resources in these systems. Ultracold atoms in optical lattices are currently highly controllable systems. Of course, the nature of lattice fermions should be chosen carefully, based on both the experimental considerations and the desired theoretical approach for lattice fermions, as discussed above.
- (ii) *The theory must be Lorentz invariant* - i.e., to have a causal structure, as a field theory. This may seem problematic, but one can simulate the lattice gauge theories described above, that obtain this symmetry in the continuum limit. This goes along quite well with the structure of the simulating systems, which are optical lattices.
- (iii) *The theory must have local gauge invariance*, which is the symmetry responsible for gauge-matter interactions. This seems the most problematic demand, and the biggest challenge, as this does not seem to be a fundamental symmetry in such atomic systems, and has been one of the most important research steps.

Thus, after considering these three requirements and recognizing that ultracold atoms in optical lattices should enable their fulfillment, such systems have been chosen as the simulating systems - building blocks for optical realizations of lattice gauge theories, opening the way to quantum simulations of lattice gauge theories. The main idea is to obtain the gauge invariant interactions which are not fundamental for ultracold atoms. We present two methods for that - one in which gauge invariance is imposed as a constraint - the effective method, in which the gauge invariance is only an emerging, low-energy sector symmetry, and the other one, in which gauge invariance is mapped into a fundamental symmetry of the atoms - conservation of hyperfine angular momentum in atomic collisions.

In all the simulation approaches presented below, regardless of the specific implementation and representation of the gauge degrees of freedom, they are

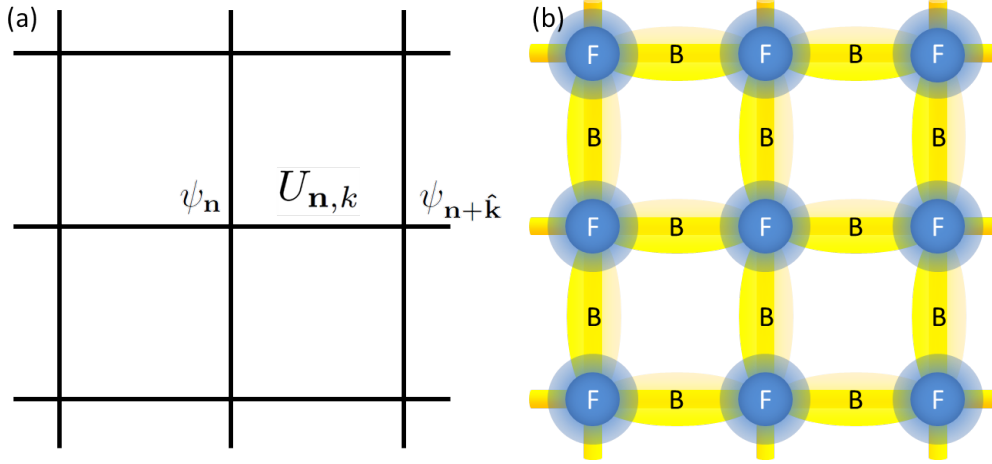


Figure 5. (a) The lattice structure. The gauge degrees of freedom occupy the links, whereas the fermionic matter - the vertices. This structure is kept in the atomic quantum simulator - whose schematic plot is presented in (b): the circles and ellipses represent the minima of the optical potentials - Bosonic (B, yellow) on the links, and Fermionic (F, blue) on the vertices.

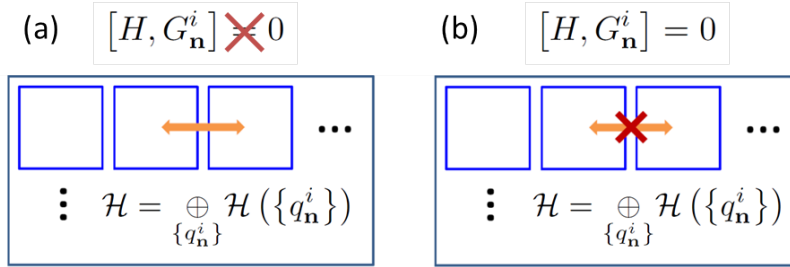


Figure 6. Effective gauge invariance. The original atomic Hamiltonian (a) mixes among the Hilbert space sectors of different static charge configurations, as it is not gauge invariant: the generators of gauge transformations (31) do not commute with the Hamiltonian. Using the Gauss's law constraint (115), one effectively eliminates the transitions among these sectors, resulting in the desired gauge invariant interactions, and the restoration of gauge invariance (10) by constructing an effective Hamiltonian to such a sector of interest.

represented by bosons populating the links of an optical lattice. Fermions, in proposals involving dynamical matter, are always located in minima coinciding with the vertices (see figure 5b).

5. Effective gauge invariance emerging at low energies

First we shall describe a class of models, in which the gauge symmetry is not fundamental, but rather arises in a low energy sector, as an emerging, effective symmetry. In this method, the atomic Hamiltonian is not gauge invariant, but rather contains a large penalty term, demanding, as a low energy constraint, that Gauss's

law will be satisfied. The constraint Hamiltonian takes the form

$$H_G = \lambda \sum_{\mathbf{n}} G_{\mathbf{n}}^2 \quad (115)$$

where λ is the largest energy scale in the system. This automatically divides the physical Hilbert space into sectors, corresponding to different eigenvalues of $G_{\mathbf{n}}$ (31) - different static charge configurations, but the Hamiltonian interactions involve transitions among them. These are practically impossible, due to energy conservation. Thus, an effective Hamiltonian [193, 194] for the ground sector has been introduced in any of these proposals, giving rise to a gauge-invariant effective theory, which includes the desired interaction (see figure 6).

5.1. *cQED in 2 + 1 dimensions - link interactions*

It is shown in [127], as a proof of principle, that a quantum simulation of the Kogut-Susskind Hamiltonian for *cQED* is, indeed, possible, and this was the first work arguing that. This first proposal discussed only the pure-gauge theory, suggesting a method to observe confinement of static charges, by probing electric flux tubes.

In this work, every link of a two-dimensional spatial lattice (labeled by the vertex from each it emanates (m, n) and its direction k) is occupied by a Bose-Einstein condensate, with a mean number of atoms N_0 (uniform all over the lattice). We expand the local number operators $N_{m,n}^k$,

$$N_{m,n}^k = N_0 + \delta_{m,n}^k \quad (116)$$

where N_0 is a C-number and $\delta_{m,n}^k$ - an operator, measuring the excess of the atomic population over (or below) N_0 , which can take negative values as well - and represents the electric field. These operators are conjugate to the local condensates' phases, $\theta_{m,n}^k$, playing the role of the compact vector potential.

In a limit where the expectation value, as well as the uncertainty of $\delta_{m,n}^k$ are much smaller than N_0 , a quantum-rotor approximation may be introduced, allowing the expansion of local annihilation (or creation) operators as

$$a \approx \sqrt{N_0} e^{i\theta} \quad (117)$$

Neighboring links are populated by condensates of different atomic species, and thus direct, gauge-variant tunneling is eliminated. This is possible by the use of holographic masks, for example, for the creation of the optical lattice. Local scattering processes are responsible to the electric Hamiltonian, as well as, along with neighboring links scattering, Gauss's law constraint. Using external lasers, desired hopping processes between neighboring links (diagonally) are introduced (see figure 7). These terms are gauge-variant as well, but they induce effective gauge invariance: these hopping processes correspond to violation of the constraint, but second-order perturbation theory ties pairs of them together, forming the plaquette interactions (see figure 8).

Experimental considerations (homogeneity of the scattering lengths) result in a sum-Gauss's law, rather than with a divergence, i.e.,

$$G_{m,n} = \delta_{m,n}^1 + \delta_{m,n}^2 + \delta_{m-1,n}^1 + \delta_{m,n-1}^2 - \Delta_{m,n} \quad (118)$$

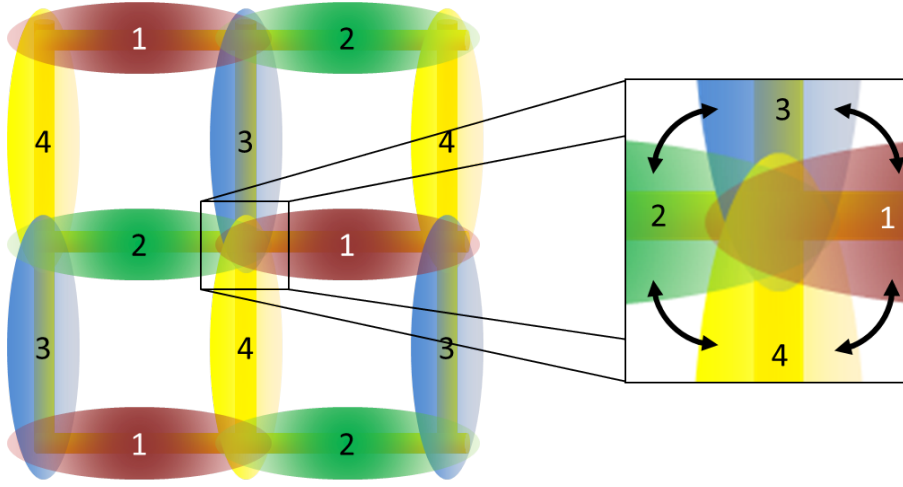


Figure 7. The lattice structure of [127]. Bosons of four different species (1-4) occupy the links such that neighboring links are occupied by different species, and thus nearest-neighbor hopping is avoided. Instead, diagonal hopping processes are induced by external lasers (denoted by black arrows on the right): $1 \leftrightarrow 3, 3 \leftrightarrow 2, 2 \leftrightarrow 4, 4 \leftrightarrow 1$. Scattering processes take place among the four species meeting in (and overlapping on) a vertex, and must be tailored properly.

and thus a (theoretical) canonical transformation, involving inversion of signs, must be carried out in order to obtain the “right” *cQED* degrees of freedom,

$$E_{m,n}^k = (-1)^{m+n} \delta_{m,n}^k; \theta_{m,n}^k \longrightarrow (-1)^{m+n} \theta_{m,n}^k; q_{m,n} = (-1)^{m+n} \Delta_{m,n} \quad (119)$$

Being theoretical, this transformation should be carried out on the results of the measurements: a strong coupling electric flux-tube will thus be manifest by a line of *alternating* values of $\delta_{m,n}^k$ between the charges.

This proposal also allows leaving the perturbative (in terms of the simulated theory) strong-coupling regime, but to a limited extent, since the atomic excess must be small comparing to the mean population, which cannot be too large due to experimental consequences. However, in 2+1 dimensions, where confinement holds also in the weak limit, the simulation of the weak limit should work - at least qualitatively, even if not describing the exact weak limit of the full Kogut-Susskind Hamiltonian. This can be understood from the weak limit analysis of [128].

5.2. Truncated *cQED* model - link interactions

The second proposal [128] was a first step in the direction of a simpler implementation. Instead of Bose-Einstein condensates, each link is occupied by a single atom, belonging to each of $2\ell + 1$ possible atomic species, representing $2\ell + 1$ possible values of the electric field on a link: Here we have introduced the *spin-gauge* model, in which the electric field is truncated (taking values between $-\ell$ and ℓ), but the gauge symmetry is unaffected, which should lead, at least qualitatively, to similar effects those of as the Kogut-Susskind Hamiltonian. The $U(1)$ angular momenta are replaced by $SU(2)$ angular momenta in an integer representation ℓ with $2\ell + 1$ levels, with the L operators of the electric field replaced by the truncated L_z , and the unitary raising/lowering

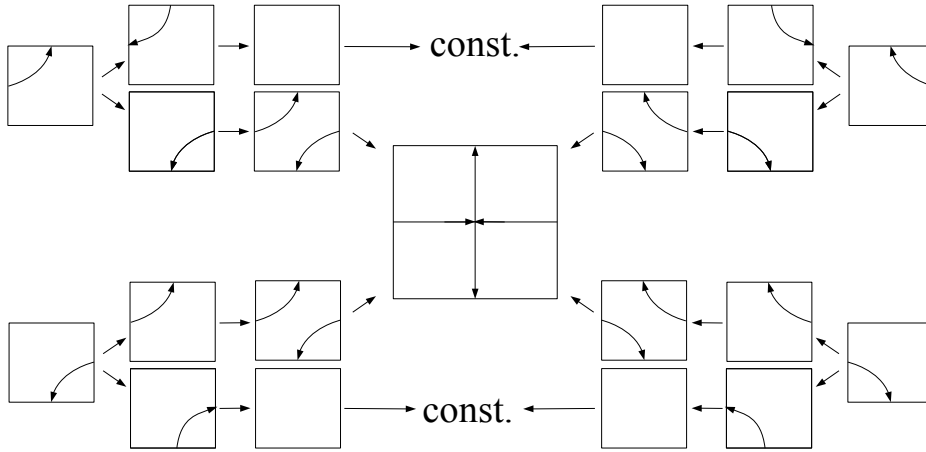


Figure 8. Generation of plaquette interactions as effective second-order terms, as in [127]. First, an atom hops from a link to a neighboring one (diagonally). Then the Gauss constraint (115) is violated, and a second process, restoring the constraint, must take place. This may either be another hopping process, with other two links, closing a plaquette, or the inverse hopping which results in “canceling” the first one, resulting in a constant term in the approach of [127] (and in other gauge-invariant terms in the spin-gauge approach [128], where the link operators are not unitary). Each plaquette is constructed out of four different second order processes. Note that the arrows correspond to the “modified Gauss’s law” (118), with opposite signs on half of the links - i.e. to the language of the simulating systems (atoms) and not to the “right signs” of $cQED$, obtained after the canonical transformation (119).

phase operators replaced by the non-unitary $SU(2)$ ladder operators L_{\pm} :

$$U \rightarrow \frac{1}{\sqrt{\ell(\ell+1)}} L_+ \quad (120)$$

in a confining phase, the electric field is supposed to take small values m , and thus with a large enough ℓ , as well as the $m \ll \ell$ of confinement, the unitarity of the ladder operators is approximately restored, at least in the sense that when one acts with them on the $|\ell m\rangle$ states, no prefactor is obtained:

$$\frac{1}{\sqrt{\ell(\ell+1)}} L_{\pm} |\ell m\rangle = \sqrt{1 - \frac{m(m \pm 1)}{\ell(\ell+1)}} |\ell, m \pm 1\rangle \approx |\ell, m \pm 1\rangle \quad (121)$$

In this representation, one obtains the *Spin-Gauge Hamiltonian* [128],

$$H_{SG} = \frac{g^2}{2} \sum_{\mathbf{n}, k} L_{z, \mathbf{n}, k}^2 - \frac{1}{2g^2 \ell^2 (\ell+1)^2} \sum_{\text{plaquettes}} \left(L_{+, \mathbf{n}, 1} L_{+, \mathbf{n}+\hat{1}, 2} L_{-, \mathbf{n}+\hat{2}, 1} L_{-, \mathbf{n}, 2} + H.c. \right) \quad (122)$$

We have compared this model to the Kogut-Susskind Hamiltonian (37). First, we have shown the more obvious result, that in the strong limit, as the states are eigenstates of electric flux (see subsection 2.4.2), one may use a truncated theory which suffices to describe the state of the system in the presence of static charges.

Conditions on ℓ , depending on the magnitude of the static charges, have been discussed using perturbation theory considerations. It was shown what is the highest order in strong-limit perturbation theory, in which the spin-gauge states will correspond to the Kogut-Susskind ones, for a given charge configuration.

Furthermore, we have addressed the nonperturbative, nontrivial weak limit as well, and compared numerically the single-plaquette results for a truncated Kogut-Susskind theory as well as the spin gauge theory to the analytical results of [108]. The results converge quantitatively to the analytical ones very quickly - for small values of ℓ (already for $\ell \sim 2, 3$).

An implementation for $\ell = 1$ - three bosonic internal levels - has been introduced. It involves a three-scale hierarchy - the first, strongest constraint is responsible to the effective "angular-momentum" interactions [195] and the second one to gauge invariance, in a similar manner to [127]. Working with $\ell = 1$ limits the possibility of going into the weak limit. Nevertheless, the rapid convergence of the results in the weak limit to the ones of the Kogut-Susskind model, do show that implementations of the spin-gauge model for higher values of ℓ shall serve as an accurate weak-limit simulation. Confinement and flux tubes take place here in the form of alternating atomic species along the line connecting the static charges - in the strong limit.

Due to the non-unitarity of the L_{\pm} operators, the effective constructions involves some undesired terms. However, they are gauge-invariant as well (as they satisfy Gauss's law constraint) and their effect is discussed in [128].

Finally, in [133], we have introduced dynamical fermions as well. Still considering $cQED$, in the spin-gauge model presented in paper [128], but regardless of the implementation the gauge degrees of freedom, we have introduced naive fermions into the system, in 2+1 dimensions.

Working with naive fermions in two spatial dimensions, each vertex contains two fermionic species, simulating a 2-component Dirac spinor,

$$\psi_{\mathbf{n}} = \begin{pmatrix} c_{\mathbf{n}} \\ d_{\mathbf{n}} \end{pmatrix} \quad (123)$$

with the local charge

$$Q_{\mathbf{n}} = \psi_{\mathbf{n}}^{\dagger} \psi_{\mathbf{n}} - 1 = N_{\mathbf{n}}^C + N_{\mathbf{n}}^D - 1 \quad (124)$$

(similarly to the charge in the second quantized Dirac field. There, for the lower entry of the spinor, we swap the fermionic creation and annihilation operators, and thus obtain that this charge transforms to the well known $N_{\mathbf{n}}^C - N_{\mathbf{n}}^D$ form).

The simulated Hamiltonian (besides the pure-gauge part, (122)) in 2+1 dimensions, is

$$H_{naive} = \frac{i\epsilon}{\sqrt{\ell(\ell+1)}} \sum_{\mathbf{n},k} (\psi_{\mathbf{n}}^{\dagger} \sigma_k \psi_{\mathbf{n}+\hat{\mathbf{k}}} L_{+,n,k} - H.c.) + M \sum_{\mathbf{n},k} \psi_{\mathbf{n}}^{\dagger} \sigma_z \psi_{\mathbf{n}} \quad (125)$$

with the Dirac matrices being Pauli matrices, $\alpha_{1,2} = \sigma_{x,y}$ and $\beta = \sigma_z$. The fermionic mass terms manifest explicitly that the particles and antiparticles are not divided among vertices as in the staggered formulation.

Gauge invariance is still effective here. Inclusion of dynamical charges into the Gauss's law constraints made it harder to implement, requiring also alternating signs to the dynamical charges. A detailed prescription for the implementation, based on fermion-boson scattering, was given, enabling the generation of this required constraint

- the interaction between the gauge field and the matter arises as an effective second order term as well: in order to satisfy the constraint, fermions can only hop along with a change of the electric field on the link.

Generalization of this method to other types of lattice fermions is straightforward. One simply has to change the fermionic ingredients and tailor the desired hopping. The effective construction will "make sure" that only the gauge-invariant interactions are obtained.

5.3. *Effective Gauge Invariance - some general remarks*

The three proposals [127, 128, 133] involved gauge invariance as an effective symmetry. This allows introducing gauge invariance to the simulating systems, but it is not the only possible approach, as shown in the subsequent papers [121, 146].

The Gauss's law constraint involves scattering of atoms, representing the gauge field degrees of freedom, on several neighboring links. All the interactions must be with the same amplitude, which is hard to implement. This may lead to practical impossibilities to satisfy the Gauss's law, for example, or to the unintended inclusion of fractional charges.

The robustness of this method was considered by Kasamatsu et. al. [196, 197], who showed, mainly based on [127] but also on other works of us and the other groups, that one may relax the fine-tuning demands of the simulating Hamiltonian parameters, and still get a gauge-invariant theory, involving Higgs fields.

Another disadvantage of this approach applies to simulation of non-Abelian gauge theories. There, the generators of gauge transformations, required for the Gauss's law constraint, are much more complicated (several non-commuting generators (31)), which makes the constraint Hamiltonian (115) very difficult to realize.

6. Local gauge invariance arising from many body interaction symmetries

The basic idea of the second simulation approach we describe hereby, is that one could use local interactions of the many body system - atomic collisions - to achieve local gauge invariance. In particular, we have utilized the conservation of the hyperfine angular momentum in atomic collisions. This enables to obtain, as fundamental ingredients of the Hamiltonian, the on-link gauge-matter (boson-fermion) interactions of (9), without any constraints or perturbation theory [121, 146]. As a second step, in $2 + 1$ (and more) dimensional setups, one may introduce the *loop method* [121] presented below, which allows the construction of the plaquette interactions effectively, but out of the *already gauge invariant* on-link interactions.

The basic, on-link interactions (9) are obtained from boson-fermion collisions, utilizing the overlap of four Wannier functions on a link (two bosonic on the links and two fermionic on its edges). The only allowed scattering channels are those which conserve the hyperfine angular momentum. Thus, one can specifically choose the hyperfine levels playing the roles of the different *simulated* bosons and fermions, such that the F conserving processes will be mapped to the gauge invariant ones. This gives us the desired interactions, along with other ones, gauge invariant as well, which may be tolerated or tamed.

6.1. Compact QED - on-link interactions

We shall show this procedure in detail for compact QED in 1+1 dimensions - the lattice Schwinger model. Besides its advantage as a "toy model" which allows a clear and simple presentation of the method, the quantum simulation of 1+1 dimensional QED with matter, in the manner presented below, has several advantages:

- (i) As gauge invariance is fundamental here, no use of effective interactions is required - i.e., the simulating Hamiltonian produces the simulated theory without any use of perturbation theory. This implies that the energy scales are larger, and thus the simulation should be faster and more robust to noise and decoherence.
- (ii) It is a possibly simpler implementation (compared with [127] and [128]).
- (iii) The 1+1 dimensional Schwinger model is exactly solvable [102, 103]. Lattice results are available as well ([171] and much more, including new calculations involving matrix product states [172]). Along with 3, this make this model a possibly preferred model for a first physical realization, as one has analytical and numerical results to compare with.

While the fermions are simply fermionic atoms in this simulation (staggered ones, to be specific, but they may be generalized to other lattice fermion representations), the bosonic fields are constructed out of the so-called *Schwinger bosons*, utilizing Schwinger's representation of $SU(2)$ [198, 199]: In this *cQED* simulation, each link may be populated by two different bosonic species, a and b , from which the algebra is constructed in the following way:

$$L_z = \frac{1}{2} (a^\dagger a - b^\dagger b) \quad ; \quad \ell = \frac{1}{2} (a^\dagger a + b^\dagger b) \quad (126)$$

$$L_+ = a^\dagger b \quad ; \quad L_- = b^\dagger a \quad (127)$$

using this representation, along with the conservation of hyperfine angular momentum, simulations of the spin-gauge Hamiltonian may be obtained, but much simply than in the effective approach. Assuming that the bosons do not interact among links, ℓ is fixed and governed by the number of on-link bosons. If we consider a single link, whose left edge may be occupied only by the fermionic species c , and its right edge by d , we wish to obtain the interactions

$$c^\dagger L_+ d + d^\dagger L_- c = c^\dagger a^\dagger b d + d^\dagger b^\dagger a c \quad (128)$$

and this is possible by selecting

$$m_F(a) + m_F(c) = m_F(b) + m_F(d) \quad (129)$$

(see figure 9). Even two atoms per link, equivalent to $\ell = 1$, give rise to the required gauge symmetry. But enlarging ℓ here involves many atoms of the same two species - condensates - rather than many degrees of freedom, as in [128]. The electric energy term of L_z^2 is obtained by other "gauge invariant" scattering processes, between the bosons of a single link.

This simulation proposal has been treated numerically, using matrix product states [174].

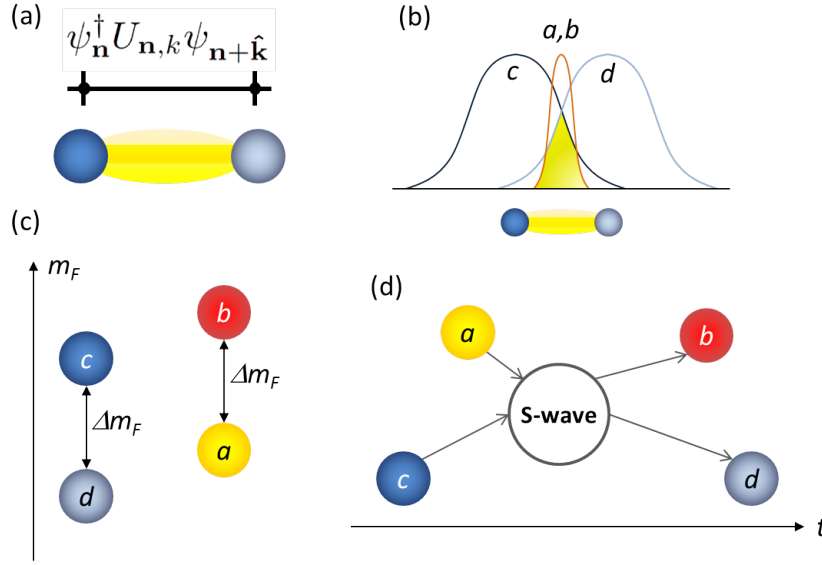


Figure 9. "Exact gauge invariance" - the Schwinger model example. (a) The desired interactions (9) are obtained as the F preserving boson-fermion scattering processes, utilizing the overlap of bosonic and fermionic Wannier functions on the link (b). By appropriately choosing the hyperfine levels representing the bosons and the fermions (c), only the gauge invariant interactions (128) of (113) are possible (d).

6.2. $SU(2)$ - Yang Mills theory - on-link interactions

6.2.1. Left and right Schwinger representations. One can utilize this type of interactions for other gauge theories as well, such as the $SU(2)$ lattice gauge theory. In [146], we have suggested a way for realizing an $SU(2)$ lattice gauge theory, in $1+1$ dimensions, utilizing the prepotential method [140, 141, 142, 143] for representing the gauge degrees of freedom (which generalizes the Schwinger representation). In this method, every link is decomposed into two parts - left and right, corresponding to the left and right degrees of freedom. The Hilbert space of each edge of the link consists of two harmonic oscillators, generating a separate Schwinger algebra: $a_{1,2}$ on the left side, with the left $SU(2)$ algebra (24) generated by

$$L_\alpha = \frac{1}{2} \sum_{ij} a_i^\dagger (\sigma_\alpha)_{ji} a_j \quad (130)$$

and $b_{1,2}$ on the right side, with the right $SU(2)$ (25) algebra generated by

$$R_\alpha = \frac{1}{2} \sum_{ij} b_i^\dagger (\sigma_\alpha)_{ij} b_j \quad (131)$$

The left and right couples of oscillators have the same total number of excitations -

$$N_L \equiv a_1^\dagger a_1 + a_2^\dagger a_2 = b_1^\dagger b_1 + b_2^\dagger b_2 \equiv N_R \quad (132)$$

(which is proportional to the total angular momentum in the Schwinger representation (126)), and thus, relation (60) is satisfied and the correct Hilbert space, with three

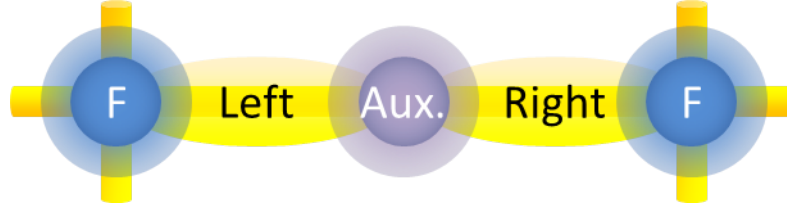


Figure 10. Structure of the non-Abelian lattice atomic simulator in the prepotential method: the simulated link is decomposed into two pieces, tied together by an auxiliary fermion.

degrees of freedom and left and right $SU(2)$ algebras, is achieved. The rotation matrices' elements are constructed out of creation and annihilation operators of these oscillators. One can decompose them to $U = U_L U_R$, with the matrices

$$U_L = \frac{1}{\sqrt{N_L + 1}} \begin{pmatrix} a_1^\dagger & -a_2 \\ a_2^\dagger & a_1 \end{pmatrix}; U_R = \begin{pmatrix} b_1^\dagger & b_2^\dagger \\ -b_2 & b_1 \end{pmatrix} \frac{1}{\sqrt{N_R + 1}} \quad (133)$$

defined on both sides of the link.

The implementation presented in [146] involves bosons on the links and fermions on the vertices, as before, but now, due to the new, exact gauge invariance method, the hyperfine levels of the atoms must be chosen carefully, such that only the desired scattering processes, which correspond to gauge invariant interaction, will be allowed by hyperfine angular momentum conservation. The links were not established as "first principle interactions", but rather "glued" out of two building blocks, using auxiliary, ancillary fermions, in second order perturbation theory, forming effective link interactions: each of the building blocks is obtained using the above prescription, involving transition to the auxiliary fermionic site in the middle, whose energy is too high, and in order to satisfy this constraint, one obtains, in second order, the full $SU(2)$ link (see figure 10). Nevertheless, gauge invariance is not effective in this proposal in the sense there is no Gauss's law constraint, and this is the achievement of this work. The link bosons involved contain four species playing the role of the harmonic oscillators of the prepotential method, from which the algebras are constructed, and other four "auxiliary" species, serving as "reference baths" required for the number-conserving scattering processes.

However, this is not a simulation of the "full" $SU(2)$ Kogut-Susskind theory using the exact prepotential Hamiltonian; Much like some of the $cQED$ simulations (in the spin gauge method), in which the electric field was truncated, here it was restricted to the representations $j = 0, \frac{1}{2}$. This, along with the square roots in the denominators of prepotential representation of the group elements (rotation matrices) - that were not achieved in the simulation - have generated some inaccuracies compared to the Kogut-Susskind theory, which result in the dynamics being accurate only in a regime where one may consider the gauge-matter interactions as a small perturbation (to sixth order in it).

6.2.2. Truncation scheme for the Hilbert space of non-Abelian groups. One can overcome the problem of square roots of operators in the denominator, as well as the need for auxiliary bosonic species and decomposition of the links, if the truncation scheme of [163] is utilized. In this method, we still work with a truncated theory, but

the truncation is done in a gauge invariant way, which does not involve decomposition of the link into two (left and right) pieces.

The bosonic degrees of freedom are represented by single bosonic atoms residing on each link of the lattice. The state of each such atom may be one of $\mathcal{N} = \sum_{j=0}^{J_{max}} (2j+1)^2$ internal levels, labeled by $|jmm'\rangle$. These are generated from the local atomic vacuum state $|0\rangle$ by the creation operators $a_{mm'}^{\dagger j}$, with $j \in \{q/2\}_{q=0}^{2J_{max}}$, $-j \leq m, m' \leq j$:

$$|jmm'\rangle = a_{mm'}^{\dagger j} |0\rangle \quad (134)$$

Out of these creation operators, and their conjugate annihilation operators, one can construct the $SU(2)$ algebras

$$L_\alpha = \sum_j a_{mm'}^{\dagger j} (T_\alpha^j)_{nm} a_{nm}^j \quad R_\alpha = \sum_j a_{mm'}^{\dagger j} (T_\alpha^j)_{m'n'} a_{m'n'}^j \quad (135)$$

where a summation is assumed on double indices. T_α^j are the j th representation matrices of $SU(2)$ (for example, $T_\alpha^{1/2} = \sigma_\alpha/2$). These operators satisfy the left and right $SU(2)$ algebras presented above. Ladder operators may be defined as $L_\pm = L_x \mp iL_y = \sum_j a_{mm'}^{\dagger j} (T_\pm^j)_{mn} a_{nm}^j$ and $R_\pm = R_x \pm iR_y = \sum_j a_{mm'}^{\dagger j} (T_\pm^j)_{m'n'} a_{m'n'}^j$.

All these operators satisfy the algebras

The commutation relations with the creation operators are

$$\begin{aligned} [L_\alpha, a_{mm'}^{\dagger j}] &= (T_\alpha^j)_{mn} a_{nm}^{\dagger j} \\ [R_\alpha, a_{mm'}^{\dagger j}] &= a_{m'n'}^{\dagger j} (T_\alpha^j)_{n'm'} \end{aligned} \quad (136)$$

implying that they undergo left and right rotations within the j representation. Thus, if we perform a rotation $V \in SU(2)$ on the left and $W^\dagger \in SU(2)$ on the right, these operators will transform according to

$$a_{mm'}^{\dagger j} \rightarrow V_{mn}^j a_{nn'}^{\dagger j} W_{n'm'}^{\dagger j} \quad (137)$$

with $V^j, W^{\dagger j}$ the j th matrix representation of the group elements V, W^\dagger .

Next, one would like to exploit these transformation properties for the construction of rotation matrices - i.e., $SU(2)$ group elements. This is done, as explained for general groups in [163], using the Clebsch-Gordan series. We denote the Clebsch-Gordan coefficients by $\alpha_m^{jMN}(J, K) = \langle JjMm|KN \rangle$, and define

$$u_{mm'}^j(J, K) = \alpha_m^{jMN}(J, K) \alpha_{m'}^{jM'N'}(J, K) a_{NN'}^{\dagger K} a_{MM'}^j \quad (138)$$

The $u_{mm'}^j(J, K)$ operators undergo rotations according to the j th representation, and thus the corresponding rotation matrix elements [165] may be constructed out of them:

$$U_{mm'}^j = \sum_J \sum_{K=|J-j|}^{J+j} \sqrt{\frac{2J+1}{2K+1}} u_{mm'}^j(J, K) \quad (139)$$

However, as the $u_{mm'}^j(J, K)$ operators undergo rotations independently of each other, we can also construct objects with the desired transformation properties without

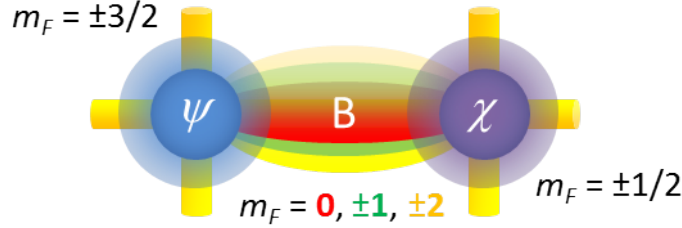


Figure 11. The simulating lattice structure. As usual, the bosonic potential's minima are on the links, and the fermionic - on the vertices. The different shapes of the bosonic minima are schematically presented.

including an infinite number of levels, i.e. with $J_{max} < \infty$. This is the result of truncating the sums in the generators and the rotation matrices, limiting them to $J \leq J_{max}$. Thus, also for a finite J_{max} one can obtain rotation matrices operating on the $j < J_{max}$ sectors, and this allows the construction of a *truncated* but yet *gauge invariant* lattice gauge theory, as we shall describe next. The unitarity is lost, and now

$$\text{tr}(U^{j\dagger}U^j) = \text{tr}(U^jU^{j\dagger}) = 2j + 1 - f_j(J_{max})P_{J_{max}} \quad (140)$$

where $P_j = \sum_{m,m'} a_{mm'}^{\dagger j} a_{mm'}^j$ is a projection operator to the j sector (recall that we are dealing with the Hilbert subspace of a single atom).

The electric Hamiltonian will simply consist of P_j projectors with the right prefactors, corresponding to linear terms in the bosonic number operators. The gauge-matter interactions are, however, more complicated.

6.2.3. Realization of the truncated on-link interactions. Next we shall give an example for the realization of the above truncation, with the $j = 0, 1/2$ representations.

The scheme we were studying contains bosons belonging to a $F = 2$ hyperfine manifold, with five different hyperfine levels (as required for $J_{max} = \frac{1}{2}$). They are prepared such that each link is populated, as required for our representation, by a single atom, and the bosonic optical wells are deep enough, such that no hopping of bosons between different bosonic sites are possible. Thus the system remains in the local single-atom Hilbert subspace. The bosonic creation operators are $\{b_m^\dagger\}$, for $-2 \leq m \equiv m_F \leq 2$. The trapping potential's minima of the different bosonic species have different shapes (generated by different internal potentials) - there are at least three different such shapes, for $|m| = 0, 1, 2$ (see figure 11). The fermions belong to an $F = 3/2$ manifold, with four different hyperfine levels. These are required for the mapping between F conservation in atomic collisions and gauge invariance. Each vertex (fermionic site) may be occupied by two fermions at most, and in an alternating manner: the even sites may be occupied by $m_F = \pm 3/2$ fermions, while the odd ones by $m_F = \pm 1/2$ only. We label even vertices' fermions by ψ and the odd by χ , where $m_F(\psi_1) = -3/2$, $m_F(\psi_2) = 3/2$, $m_F(\chi_1) = 1/2$, and $m_F(\chi_2) = -1/2$. The fermionic sites are designed such that the fermionic wavefunctions of the two edges of a link will overlap on the middle on the link, also with the bosonic wavefunctions (see figure 11).

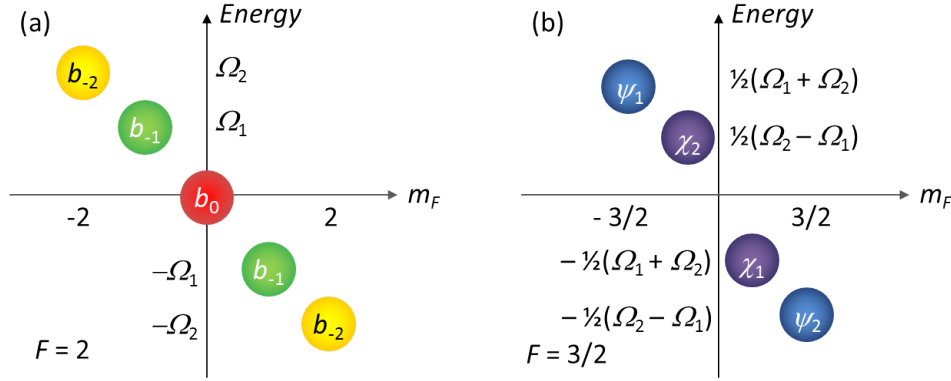


Figure 12. The energy levels of the (a) $F = 2$ bosons and the (b) $F = 3/2$ fermions, as described by H_Ω .

Using lasers or magnetic fields, depending on the atomic realization, the bosons and fermions are subject to the Hamiltonian

$$\begin{aligned}
 H_\Omega = & -\sum_L \sum_{m \neq 0} \Omega_{|m|} b_m^\dagger b_m + \frac{1}{2} \sum_{V_e} (\Omega_1 + \Omega_2) (\psi_1^\dagger \psi_1 - \psi_2^\dagger \psi_2) \\
 & + \frac{1}{2} \sum_{V_o} (\Omega_1 - \Omega_2) (\chi_1^\dagger \chi_1 - \chi_2^\dagger \chi_2)
 \end{aligned} \tag{141}$$

where L is the set of links, V_e of even vertices and V_o of odd ones, and $\Omega_1 \neq \Omega_2$, $2\Omega_1 \neq \Omega_2$ (see figure 12).

Gauge invariant interactions, according to (9), are of the form $\psi^\dagger U \chi$, where U is the group element, which is a matrix of bosonic operators, as given by (139) with $j = 1/2$ and $J_{max} = 1/2$. These interactions are constructed by the on-link fermion-boson scattering. The chosen values of m_F allow only specific scattering channels, thanks to the conservation of hyperfine angular momentum. By the introduction of H_Ω and energy conservation considerations, we further reduce the number of possible scattering processes (assume $\Omega_{1,2}$ are large enough compared to the other energy scales, and perform a rotating wave approximation with respect to H_Ω). In first quantization terms, the S-wave scattering is governed by a pseudo-potential V_S whose matrix elements are

$$\begin{aligned}
 & \left\langle 2, m'_b, \frac{3}{2}, m'_f \left| V_S \right| 2, m_b, \frac{3}{2}, m_f \right\rangle = \\
 & \delta_{m'_b + m'_f, m_b + m_f} \sum_{F=\frac{1}{2}}^{\frac{7}{2}} C_F \times \left\langle 2, m'_b, \frac{3}{2}, m'_f \left| F, m'_b + m'_f \right\rangle \times \right. \\
 & \quad \left. \times \left\langle F, m_b + m_f \left| 2, m_b, \frac{3}{2}, m_f \right\rangle \right.
 \end{aligned} \tag{142}$$

(The Kronecker delta is redundant due to the Clebsch-Gordan coefficients, but is explicitly written to manifest angular momentum conservation.)

By properly choosing the C_F coefficients and the overlap integrals (by manipulating the shape of the optical potential and hence the Wannier functions)

one may obtain the required link interactions as in (139) and the electric energy as in equation (30) (which is simply a sum of bosonic number operators, using the projectors P_j defined above), as well as avoid extra interaction terms which conserve hyperfine angular momentum, but yet are not part of the desired Hamiltonian. Unfortunately, however, we have not been able, so far, either to satisfy all the required symmetries by the simulating system, or to prove it is impossible. An experimental realization might be possible for other atomic configurations, with less stringent symmetries (i.e., a different choice of atomic levels).

For the simplest configuration described above (which could be generalized to more complicated atomic systems if required), with a theoretical simulating system with the right Hamiltonian parameters, one could proceed as follows: For even links we obtain the interaction Hamiltonian

$$\epsilon \sum_{ij} \psi_i^\dagger M_{ij} \chi_j + H.c. \quad (143)$$

and for odd ones -

$$\epsilon \sum_{ij} \chi_i^\dagger M_{ij}^\dagger \psi_j + H.c. \quad (144)$$

with the bosonic matrix

$$M = \frac{1}{\sqrt{2}} \begin{pmatrix} b_2^\dagger b_0 + b_0^\dagger b_{-2} & -b_1^\dagger b_0 + b_0^\dagger b_{-1} \\ -b_{-1}^\dagger b_0 + b_0^\dagger b_1 & b_0^\dagger b_2 + b_{-2}^\dagger b_0 \end{pmatrix} \quad (145)$$

The next step is to map between the atomic degrees of freedom b_m to the ones of the simulated theory - a_{mm}^j . The mapping is as follows:

(i) For even links,

$$\begin{aligned} b_{\pm 2}^\dagger &= a_{\pm 1/2, \pm 1/2}^{\dagger 1/2} \\ b_{\pm 1}^\dagger &= -a_{\pm 1/2, \mp 1/2}^{\dagger 1/2} \\ b_0^\dagger &= a_{00}^{\dagger 0} \end{aligned} \quad (146)$$

(ii) For odd links,

$$\begin{aligned} b_{\pm 2}^\dagger &= a_{\mp 1/2, \mp 1/2}^{\dagger 1/2} \\ b_{\pm 1}^\dagger &= a_{\pm 1/2, \mp 1/2}^{\dagger 1/2} \\ b_0^\dagger &= a_{00}^{\dagger 0} \end{aligned} \quad (147)$$

Using this mapping, one obtains that $M = U$ for even links, and $M^\dagger = U$ for the odd ones (with U being the truncated rotation matrix, acting only within the 5-dimensional Hilbert space of $j = 0, \frac{1}{2}$).

Thus, if we relabel all the fermions as Ψ , we obtain the desired interaction Hamiltonian,

$$H_{int} = \frac{\epsilon}{\sqrt{2}} \sum_n (\Psi_n^\dagger U_{n,n+1} \Psi_{n+1} + H.C.) \quad (148)$$

6.3. Plaquette interactions: $d + 1$ dimensional Abelian and non-Abelian theories

The non-effective simulations may be extended to further dimensions. The nontrivial generalization is from 1+1 to 2+1 dimensions, as it involves the inclusion of the plaquette interactions. In the previous methods, which involved effective gauge invariance, these were effectively obtained out of the *gauge-variant* interactions of the original Hamiltonian, using the gauge invariance constraint. Here they are obtained effectively as well, but out of *already gauge invariant* building blocks - the on-link gauge-matter interactions, which are not effective here, which is a great advantage.

In [121], we have introduced the "loop method", which uses heavy ancillary fermions - constrained to populate only some special vertices that may move only virtually, closing loops along plaquettes, carrying the gauge degrees of freedom along the way (utilizing the on-link interactions (128)) and thus effectively forming the plaquette interactions (see figure 13). Although these interactions are obtained as fourth-order processes and might seem too weak, they are practically only second order interactions, since the perturbative series of the gauge-matter Hamiltonian contains only even orders (fermions must hop virtually across an even distance, in order to finish in a vertex in which they may stay) and thus the fourth order is the second-leading one.

One can introduce yet other fermionic species (non-constrained) to serve as "regular", dynamical fermions, on top of the ancillary static ones.

We have utilized the loop method for a 2+1 dimensional compact QED in the spin-gauge approach - plaquettes are constructed from the 1+1 dimensional link interactions, generated due to hyperfine angular momentum conservation. This included a numerical proof of principle, considering some gauge invariant but non-Kogut-Susskind corrections to the Hamiltonian, due to the effective calculation in the truncated case. It was shown that the effective Hamiltonian still gives rise to the expected spectrum regardless of these corrections in several regimes of the Hamiltonian parameter, also outside the strong coupling limit.

The loop method has also been formulated and utilized for "ideal" simulations, rather than the above described "realistic condition" $cQED$ in 2+1 dimensions. This includes "ideal" (not truncated) $cQED$, as well as $SU(N)$ gauge theory with unitary matrices (which is not realistically achieved in the current simulation method).

Finally, we shall comment on the simulation of the \mathbb{Z}_N lattice gauge theory, whose relevance to QCD confinement has been stated above. Since this theory involves finite Hilbert spaces on the links, one could, in principle, simulate the exact model, with no truncations and approximations. An explicit example for \mathbb{Z}_3 was given. Since the local Hilbert space is finite, we use different bosonic levels on each link, playing the role of the different eigenstates of the \mathbb{Z}_N P operator. The on-link interactions are with auxiliary fermions (which are not real \mathbb{Z}_N , and are eliminated in the loop method), which can thus be also hard-core bosons (the statistics is irrelevant). The gauge invariant operators are obtained using the conservation of hyperfine angular momentum in collisions, as before, but the challenge here is to realize the cyclic "Escher staircase" nature of the group. This is done by hybridization of atomic levels, as discussed in [121].

Dynamical fermions may be included in these simulations as well, following the formulation of [163].

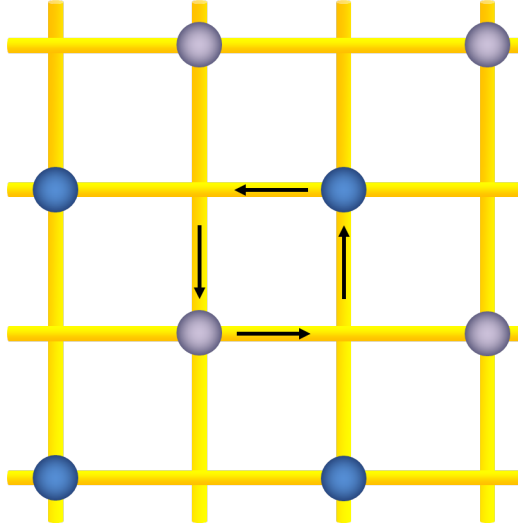


Figure 13. The loop method: Heavy, ancillary fermions (of two types, represented by the color) are constrained energetically to occupy certain vertices. Virtual loops of such fermions (as in the middle plaquette), carrying the gauge degrees of freedom along with them, generate the plaquette terms. For further details refer to [121].

6.4. Gauge invariance from atomic interaction symmetries - some general remarks

To conclude, the approach of exact gauge invariance seems to be better than the previous effective approach, as it is applicable to a larger class of models (with the loop method for the plaquette interaction, for example).

This is since it does not have to include the Gauss's law constraints, which are hard to realize (and even harder for non-Abelian gauge groups, due to the non-commuting and complicated generators) and thus this approach seems the preferred to proceed with.

Regarding the simulated theories: the simulation of $cQED$ in the non-effective approach seems closer to a physical realization than the previous, effective ones. A better physical realization of the non-Abelian models is required, in order to

- (i) Allow for a better 1+1 simulation, with no need to use perturbation theory at all (although the current realization does not rely on perturbation theory for gauge invariance, only to the generation of links).
- (ii) Include further nonperturbative regimes of 1 + 1 dimensional theories.
- (iii) Extend the simulations to 2+1 dimensions, in a way that plaquettes will be generated using the loop method even out of gauge invariant building blocks which contain non-unitary matrices; This should be possible using the truncation scheme of [163], but as explained above, a concrete physical realization is still lacking.
- (iv) Allow for simple generalizations to $SU(N)$ with $N > 2$ and further gauge groups.

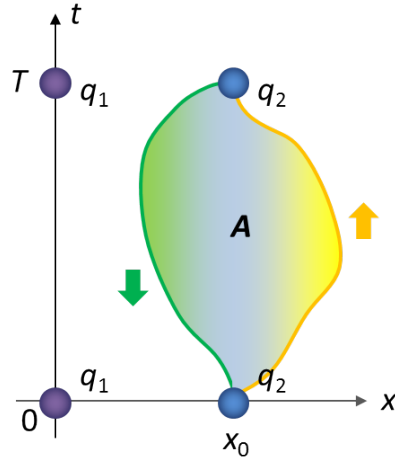


Figure 14. In the gedanken experiment presented in [200], whose realization was described in [133]. A meson, consisting of two static quarks/charges, whose length is initially x_0 , is brought into a superposition of two lengths, using two internal levels of one of them (e.g. $|\uparrow\rangle$ and $|\downarrow\rangle$) which are affected by two different potentials, and thus follow two different trajectories; At time t the two mesons in superposition are brought to the same position again, resulting again with an x_0 sized meson. After performing a Ramsey spectroscopy, within a confining phase, the probabilities for being in either of the two external states depend on the area enclosed by the trajectories A . This experiment may be used for detecting a confining phase, and within it - for measuring the string tension. For a more detailed account of this procedure, the reader may refer to [200].

7. Discussion

The class of Abelian and non-Abelian lattice gauge theories that has been considered at the present work constitutes the building blocks of the standard model of elementary particles, that currently provides us with the best known description of high-energy physics phenomena. The standard model has been so far extensively tested, and currently agrees with the experimental results from particle accelerators and cosmological observations, up to energy scales of $\sim 10^{12}\text{eV}$. On the other hand, the physics which is used here to describe the many-body system of ultra-cold atoms is well understood and has been tested with high accuracy, down to energy scales of $\sim 10^{-7}\text{eV}$: ~ 19 orders of magnitude below the energy scales of the simulated physics!

Furthermore, the difference between the simulated system and analog-simulator is not only in the energy scales: there rather exists a striking difference in the formal structure and the physical principles that govern the physics of high-energy phenomena and ultracold atoms. The atomic system at hand is non-relativistic, and seems to lack the sort of constrained symmetries and dynamical structure that are so essential for relativistic HEP models. Unlike high energy physics, atomic dynamics are number conserving, and manifest neither local gauge invariance, nor Lorentz invariance, which lead, among other things, to the familiar causal space-time structure, to charge conservation laws, to long-range interactions in QED and to quark confinement in QCD .

So the problem at hand seems conceptually not obvious: can high-energy field

theories be simulated by the physics of ultra low-energy systems?

It turns out, however and somewhat surprisingly, that there are several ways to manifest both Lorentz (as an effective long wavelength property) and local-gauge invariance. The latter can be obtained in two ways: It may arise either as a property of a low energy sector of the atomic system - hence as an effective symmetry, or, alternatively, by re-arranging the interactions such that the given low-energy symmetries of the atomic collisions are converted into a form which is equivalent to local (Abelian or non-Abelian) gauge symmetries. The first case of "effectively emerging" gauge symmetry seems to provide yet another framework to study models in which local gauge invariance is not a fundamental property of the complete theory, but rather emerges as a low energy phenomenon as suggested in [201]. The alternative "exact" mapping might, on the other hand, be more suitable for mimicking theories wherein local gauge invariance is a fundamental property.

In this report, we have reviewed recent progress on quantum simulations of lattice gauge theories using ultracold atoms, focusing on some of the works and approaches. These proposals serve as proofs of principle of the possibility to simulate high energy physics, and even gauge theories, using ultracold atoms.

Our current results already suggest that simple enough models, such as compact-QED ($U(1)$), and possibly also more involved, non-Abelian $SU(2)$ models, manifesting exotic QCD effects, (such as quark confinement) could, indeed, be experimentally studied using current table-top cold atoms experimental methods.

7.1. Advantages of quantum simulation over other approaches

- (i) As fermions "come for free" in these atomic scenarios, one may avoid the "sign problem" of Grassman integration and consider regimes of finite chemical potential, such as the exotic color-superconductivity and quark-gluon plasma phases of Quantum Chromodynamics [94, 100, 101].
- (ii) Real time dynamics is possible here, rather than in the statistical Monte-Carlo simulations (and this applies already for the current proposals). This allows, or shall allow,
 - (a) Observing real time dynamical phenomena, including the ones described in the papers: deforming and breaking of flux tubes and loops, pair creation etc.
 - (b) Changing adiabatically the Hamiltonian parameters - finding ground states of systems, by switching from "trivial" regimes where the ground state is known (e.g. no-interactions, strong limit) to other regimes; Also probing for phase transitions and creating phase diagrams of theories, depending on the theory's constants. This shall be highly relevant for *QCD* once feasible simulation systems are proposed and realized.
- (iii) Possibility to consider finite temperature models as well [93, 95, 100], including with real time dynamics .
- (iv) Possibility to realize otherwise only gedanken experiments. For example, a realization of the gedanken experiment proposed in [200], which brings the idea of Ramsey spectroscopy [202] into high energy physics, suggesting a way to probe for the confining phase and measure the string tension related with confinement (see figure 14).

7.2. Simulated models

As described in this report, a large class of Abelian and non-Abelian physical models can be simulated, including, explicitly, the lattice gauge theories of

- (i) Compact QED - Kogut Susskind and spin-gauge (truncated) models, in 1+1 and 2+1 dimensions, with both effective and exact gauge invariance, with or without dynamical matter. In 1+1 dimensions, the simulation is possible with no perturbation theory at all.
- (ii) \mathbb{Z}_N - so far, \mathbb{Z}_3 has been extensively studied - 2+1 pure gauge, or with dynamical matter (following [163]) - an exact quantum simulation of a non-truncated Hilbert space.
- (iii) $SU(N)$ - so far $SU(2)$ in 1+1 dimensions, with limited applicability to more dimensions has been studied in detail, while other $SU(N)$ groups still await extended study.

The simulatable theories, as presented in this report, are summarized in the table below, where KS - Kogut-Susskind, trunc. - truncated, st.c. - Strong coupling, YM - Yang Mills.

	1+1 with matter	2+1 Pure	2+1 with matter
$U(1)$	Full KS + trunc.	Full KS + trunc.	Full KS + trunc.
\mathbb{Z}_3	Full	Full	Full
$SU(2)$	YM + trunc.	YM + trunc. (st. c.)	YM + trunc. (st. c.)

For other \mathbb{Z}_N and $SU(N)$ groups, the simulation formalism still applies - however, experimental realizations seem highly challenging, and thus, perhaps, one should seek for other methods.

7.3. Open problems

These models and simulation proposals still require some more study, both from theoretical and experimental aspects.

On the theoretical level, it is very important to understand the implications of using truncated systems - are systems with a finite local Hilbert space accurate enough for simulations of Kogut-Susskind models, if one exploits an appropriate coarse-graining scheme? And, resulting from that, what should be the continuum limit of such theories, if it exists?

Such truncated models may be treated using tensor network techniques, and indeed, some studies approaching lattice gauge theories with tensor networks have already been carried out [172, 173, 203, 204, 174, 205, 206, 175, 176, 177, 207, 178, 208].

As far as the simulating systems are considered, the following should be studied, in order to progress on the experimental side:

- (i) Techniques for generating complex lattice and superlattice structure - both for more challenging simulation models and for increasing the number of atoms which may populate a single site.
- (ii) Improving the controllability of parameters - new ways to control scattering coefficients, for example; Also, Strengthening the possible interactions is important, for example for the realization of effective, $\sim J^2/U$, interactions, or the second $SU(2)$ realization scheme presented above, as well as, potentially, the

use of the truncation scheme of [163] for the simulation of other non-Abelian theories (with either compact Lie or finite gauge groups), including, of course $SU(3)$ for QCD .

- (iii) Methods to create longer-living and more robust lattices - cooling techniques, ways to deal with atomic losses and more.
- (iv) Measurement techniques - the current single-addressing techniques [189, 190, 191] require very sophisticated experimental methods, limited to a small number of experimental groups. Development of such, and other techniques, shall help boosting the quantum simulations of complicated physical models.

7.4. Summary

Atomic physics and high energy physics have, indeed, what to offer to one another, suggesting a very interesting and exciting physical research focusing on their interface. Reconstructing high energy physics from atomic components offers a great lesson in understanding the interactions unfolded within the standard model of particle physics. And on the broader sense, the continuation of such works on quantum simulations of high energy physics, and the growth of the community working in this direction, may lead to useful new ways, methods and results in understanding the most fundamental degrees of freedom in our physical universe.

Acknowledgements

E.Z. acknowledges the support of the Alexander-von-Humboldt Foundation. B.R. wishes to thank the hospitality of MPQ. Part of the work has been supported by the EU Integrated Project SIQS.

References

- [1] J. I. Cirac and P. Zoller. Goals and opportunities in quantum simulation. *Nat Phys*, 8(4):264–266, April 2012.
- [2] R. Feynman. Simulating physics with computers. *International Journal of Theoretical Physics*, 21(6):467–488, 1982-06-01.
- [3] S. Lloyd. Universal quantum simulators. *Science*, 273(5278):1073–1078, 1996.
- [4] C. Zalka. Simulating quantum systems on a quantum computer. *Proceedings of the Royal Society of London. Series A: Mathematical, Physical and Engineering Sciences*, 454(1969):313–322, 1998.
- [5] D. A. Lidar and O. Biham. Simulating Ising spin glasses on a quantum computer. *Phys. Rev. E*, 56:3661–3681, Sep 1997.
- [6] S. P. Jordan, K. S. M. Lee, and J. Preskill. Quantum algorithms for quantum field theories. *Science*, 336:1130–1133, 2012.
- [7] D. Jaksch, C. Bruder, J. I. Cirac, C. W. Gardiner, and P. Zoller. Cold bosonic atoms in optical lattices. *Phys. Rev. Lett.*, 81:3108–3111, Oct 1998.
- [8] M. Lewenstein, A. Sanpera, V. Ahufinger, B. Damski, A. Sen(De), and U. Sen. Ultracold atomic gases in optical lattices: mimicking condensed matter physics and beyond. *Advances in Physics*, 56(2):243–379, 2007.
- [9] I. Bloch, J. Dalibard, and W. Zwerger. Many-body physics with ultracold gases. *Rev. Mod. Phys.*, 80(3):885–964, Jul 2008.
- [10] I. Bloch, J. Dalibard, and S. Nascimbene. Quantum simulations with ultracold quantum gases. *Nat Phys*, 8(4):267–276, April 2012.
- [11] M. Lewenstein, A. Sanpera, and V. Ahufinger. *Ultracold Atoms in Optical Lattices: Simulating Quantum Many-body Systems*. Oxford University Press, 2012.
- [12] D.F.V. James. Quantum dynamics of cold trapped ions with application to quantum computation. *Applied Physics B: Lasers and Optics*, 66:181–190, 1998. 10.1007/s003400050373.

- [13] D. Leibfried, R. Blatt, C. Monroe, and D. Wineland. Quantum dynamics of single trapped ions. *Rev. Mod. Phys.*, 75:281–324, Mar 2003.
- [14] B. P. Lanyon, C. Hempel, D. Nigg, M. Mueller, R. Gerritsma, F. Zahring, P. Schindler, J. T. Barreiro, M. Rambach, G. Kirchmair, M. Hennrich, P. Zoller, R. Blatt, and C. F. Roos. Universal digital quantum simulation with trapped ions. *Science*, 334(6052):57–61, 2011.
- [15] R. Blatt and C. F. Roos. Quantum simulations with trapped ions. *Nat Phys*, 8(4):277–284, April 2012.
- [16] C. Schneider, D. Porras, and T. Schaetz. Experimental quantum simulations of many-body physics with trapped ions. *Reports on Progress in Physics*, 75(2):024401, 2012.
- [17] A. Aspuru-Guzik and P. Walther. Photonic quantum simulators. *Nat Phys*, 8(4):285–291, April 2012.
- [18] H. Weimer, M. Müller, I. Lesanovsky, P. Zoller, and H. P. Büchler. A Rydberg quantum simulator. *Nat Phys*, 6(5):382–388, May 2010.
- [19] E. Demler and F. Zhou. Spinor bosonic atoms in optical lattices: Symmetry breaking and fractionalization. *Phys. Rev. Lett.*, 88:163001, Apr 2002.
- [20] M. Greiner, O. Mandel, T. Esslinger, T. W. Hansch, and I. Bloch. Quantum phase transition from a superfluid to a Mott insulator in a gas of ultracold atoms. *Nature*, 415(6867):39–44, January 2002.
- [21] J.J. Garcia-Ripoll and J. I. Cirac. Spin dynamics for bosons in an optical lattice. *New Journal of Physics*, 5(1):76, 2003.
- [22] T. Stöferle, H. Moritz, C. Schori, M. Köhl, and T. Esslinger. Transition from a strongly interacting 1d superfluid to a Mott insulator. *Phys. Rev. Lett.*, 92:130403, Mar 2004.
- [23] D. Porras and J. I. Cirac. Effective quantum spin systems with trapped ions. *Phys. Rev. Lett.*, 92:207901, May 2004.
- [24] J. J. Garcia-Ripoll, M. A. Martin-Delgado, and J. I. Cirac. Implementation of spin hamiltonians in optical lattices. *Phys. Rev. Lett.*, 93:250405, Dec 2004.
- [25] M. Lewenstein, L. Santos, M. A. Baranov, and H. Fehrmann. Atomic Bose-Fermi mixtures in an optical lattice. *Phys. Rev. Lett.*, 92:050401, Feb 2004.
- [26] D. Jaksch and P. Zoller. The cold atom Hubbard toolbox. *Annals of Physics*, 315(1):52 – 79, 2005. Special Issue.
- [27] J. Wehr, A. Niederberger, L. Sanchez-Palencia, and M. Lewenstein. Disorder versus the Mermin-Wagner-Hohenberg effect: From classical spin systems to ultracold atomic gases. *Phys. Rev. B*, 74:224448, Dec 2006.
- [28] M. Ortner, A. Micheli, G. Pupillo, and P. Zoller. Quantum simulations of extended Hubbard models with dipolar crystals. *New Journal of Physics*, 11(5):055045, 2009.
- [29] J. W. Britton, B. C. Sawyer, A. C. Keith, C.-C. J. Wang, J. K. Freericks, H. Uys, M. J. Biercuk, and J. J. Bollinger. Engineered two-dimensional ising interactions in a trapped-ion quantum simulator with hundreds of spins. *Nature*, 484(7395):489–492, Apr 2012.
- [30] M. Endres, T. Fukuhara, D. Pekker, M. Cheneau, P. Schauss, C. Gross, E. Demler, S. Kuhr, and I. Bloch. The "Higgs" amplitude mode at the two-dimensional superfluid/Mott insulator transition. *Nature*, 487(7408):454–458, July 2012.
- [31] D. Jaksch and P. Zoller. Creation of effective magnetic fields in optical lattices: the Hofstadter butterfly for cold neutral atoms. *New Journal of Physics*, 5(1):56, 2003.
- [32] E. J. Mueller. Artificial electromagnetism for neutral atoms: Escher staircase and Laughlin liquids. *Phys. Rev. A*, 70:041603, Oct 2004.
- [33] A. S. Sorensen, E. Demler, and M. D. Lukin. Fractional quantum Hall states of atoms in optical lattices. *Phys. Rev. Lett.*, 94:086803, Mar 2005.
- [34] K. Osterloh, M. Baig, L. Santos, P. Zoller, and M. Lewenstein. Cold atoms in non-abelian gauge potentials: From the Hofstadter "moth" to lattice gauge theory. *Phys. Rev. Lett.*, 95:010403, Jun 2005.
- [35] J. Ruseckas, G. Juzeliunas, P. Ohberg, and M. Fleischhauer. Non-abelian gauge potentials for ultracold atoms with degenerate dark states. *Phys. Rev. Lett.*, 95:010404, Jun 2005.
- [36] G. Juzeliunas, J. Ruseckas, A. Jacob, L. Santos, and P. Ohberg. Double and negative reflection of cold atoms in non-abelian gauge potentials. *Phys. Rev. Lett.*, 100:200405, May 2008.
- [37] B. Paredes and I. Bloch. Minimum instances of topological matter in an optical plaquette. *Phys. Rev. A*, 77:023603, Feb 2008.
- [38] N. Goldman, A. Kubasiak, P. Gaspard, and M. Lewenstein. Ultracold atomic gases in non-abelian gauge potentials: The case of constant Wilson loop. *Phys. Rev. A*, 79:023624, Feb 2009.
- [39] O. Boada, A. Celi, J.I. Latorre, and V. Pico. Simulation of gauge transformations on systems of ultracold atoms. *New Journal of Physics*, 12(11):113055, 2010.

- [40] E. Alba, X. Fernandez-Gonzalvo, J. Mur-Petit, J. K. Pachos, and J. J. Garcia-Ripoll. Seeing topological order in time-of-flight measurements. *Phys. Rev. Lett.*, 107:235301, Nov 2011.
- [41] M. Aidelsburger, M. Atala, M. Lohse, J. T. Barreiro, B. Paredes, and I. Bloch. Realization of the Hofstadter Hamiltonian with ultracold atoms in optical lattices. *Phys. Rev. Lett.*, 111:185301, Oct 2013.
- [42] H. Miyake, G. A. Siviloglou, C. J. Kennedy, W. C. Burton, and W. Ketterle. Realizing the Harper Hamiltonian with laser-assisted tunneling in optical lattices. *Phys. Rev. Lett.*, 111:185302, Oct 2013.
- [43] S. W. Hawking. Black hole explosions? *Nature*, 248, Mar 1974.
- [44] W. G. Unruh. Notes on black-hole evaporation. *Phys. Rev. D*, 14:870–892, Aug 1976.
- [45] L. J. Garay, J. R. Anglin, J. I. Cirac, and P. Zoller. Sonic black holes in dilute Bose-Einstein condensates. *Phys. Rev. A*, 63:023611, Jan 2001.
- [46] C. Barcelo, S. Liberati, and M. Visser. Analogue gravity from Bose-Einstein condensates. *Classical and Quantum Gravity*, 18(6):1137, 2001.
- [47] U. R. Fischer and R. Schützhold. Quantum simulation of cosmic inflation in two-component Bose-Einstein condensates. *Phys. Rev. A*, 70:063615, Dec 2004.
- [48] M. Visser and S. Weinfurter. Massive Klein-Gordon equation from a Bose-Einstein-condensation-based analogue spacetime. *Phys. Rev. D*, 72:044020, Aug 2005.
- [49] A. Retzker, J. I. Cirac, M. B. Plenio, and B. Reznik. Methods for detecting acceleration radiation in a Bose-Einstein condensate. *Phys. Rev. Lett.*, 101:110402, Sep 2008.
- [50] B. Horstmann, B. Reznik, S. Fagnocchi, and J. I. Cirac. Hawking radiation from an acoustic black hole on an ion ring. *Phys. Rev. Lett.*, 104:250403, Jun 2010.
- [51] O. Lahav, A. Itah, A. Blumkin, C. Gordon, S. Rinott, A. Zayats, and J. Steinhauer. Realization of a sonic black hole analog in a Bose-Einstein condensate. *Phys. Rev. Lett.*, 105:240401, Dec 2010.
- [52] B. Horstmann, R. Schützhold, B. Reznik, S. Fagnocchi, and J. I. Cirac. Hawking radiation on an ion ring in the quantum regime. *New Journal of Physics*, 13(4):045008, 2011.
- [53] R. Schley, A. Berkovitz, S. Rinott, I. Shammass, A. Blumkin, and J. Steinhauer. Planck distribution of phonons in a Bose-Einstein condensate. *Phys. Rev. Lett.*, 111:055301, Jul 2013.
- [54] L. Lamata, J. León, T. Schätz, and E. Solano. Dirac equation and quantum relativistic effects in a single trapped ion. *Phys. Rev. Lett.*, 98:253005, Jun 2007.
- [55] J. Y. Vaishnav and Charles W. Clark. Observing Zitterbewegung with ultracold atoms. *Phys. Rev. Lett.*, 100:153002, Apr 2008.
- [56] R. Gerritsma, G. Kirchmair, F. Zahringer, E. Solano, R. Blatt, and C. F. Roos. Quantum simulation of the Dirac equation. *Nature*, 463(7277):68–71, January 2010.
- [57] R. Gerritsma, B. P. Lanyon, G. Kirchmair, F. Zahringer, C. Hempel, J. Casanova, J. J. Garcia-Ripoll, E. Solano, R. Blatt, and C. F. Roos. Quantum simulation of the Klein paradox with trapped ions. *Phys. Rev. Lett.*, 106:060503, Feb 2011.
- [58] E. Zohar and B. Reznik. The Fermi problem in discrete systems. *New Journal of Physics*, 13(7):075016, 2011.
- [59] C. Sabin, M. del Rey, J. J. Garcia-Ripoll, and J. Leon. Fermi problem with artificial atoms in circuit QED. *Phys. Rev. Lett.*, 107:150402, Oct 2011.
- [60] C. Noh, B. M. Rodriguez-Lara, and A. G. Angelakis. Quantum simulation of neutrino oscillations with trapped ions. *New Journal of Physics*, 14(3):033028, 2012.
- [61] J. Casanova, C. Sabin, J. Leon, I. L. Egusquiza, R. Gerritsma, C. F. Roos, J. J. Garcia-Ripoll, and E. Solano. Quantum simulation of the Majorana equation and unphysical operations. *Phys. Rev. X*, 1:021018, Dec 2011.
- [62] C. Noh, B. M. Rodriguez-Lara, and D. G. Angelakis. Proposal for realization of the Majorana equation in a tabletop experiment. *Phys. Rev. A*, 87:040102, Apr 2013.
- [63] B. Reznik. Entanglement from the vacuum. *Foundations of Physics*, 33(1):167–176, 2003.
- [64] A. Retzker, J. I. Cirac, and B. Reznik. Detecting vacuum entanglement in a linear ion trap. *Phys. Rev. Lett.*, 94:050504, Feb 2005.
- [65] J. I. Cirac, P. Maraner, and J. K. Pachos. Cold atom simulation of interacting relativistic quantum field theories. *Phys. Rev. Lett.*, 105:190403, Nov 2010.
- [66] A. Bermudez, L. Mazza, M. Rizzi, N. Goldman, M. Lewenstein, and M. A. Martin-Delgado. Wilson fermions and axion electrodynamics in optical lattices. *Phys. Rev. Lett.*, 105:190404, Nov 2010.
- [67] O. Boada, A. Celi, J. I. Latorre, and M. Lewenstein. Dirac equation for cold atoms in artificial curved spacetimes. *N. J. of Phys.*, 13(3):035002, 2011.
- [68] L. Mazza, A. Bermudez, N. Goldman, M. Rizzi, M. A. Martin-Delgado, and M. Lewenstein.

- An optical-lattice-based quantum simulator for relativistic field theories and topological insulators. *N. J. of Phys.*, 14(1):015007, 2012.
- [69] N. Szpak and R. Schützhold. Optical lattice quantum simulator for quantum electrodynamics in strong external fields: spontaneous pair creation and the Sauter-Schwinger effect. *New Journal of Physics*, 14(3):035001, 2012.
- [70] O. Boada, A. Celi, J. I. Latorre, and M. Lewenstein. Quantum simulation of an extra dimension. *Phys. Rev. Lett.*, 108:133001, Mar 2012.
- [71] Octavi Boada, Alessio Celi, Maciej Lewenstein, Javier Rodríguez-Laguna, and José I Latorre. Quantum simulation of non-trivial topology. *arXiv preprint arXiv:1409.4770*, 2014.
- [72] Y Yu and K Yang. Supersymmetry and the goldstino-like mode in Bose-Fermi mixtures. *Phys. Rev. Lett.*, 100:090404, Mar 2008.
- [73] T. Shi, Yue Yu, and C. P. Sun. Supersymmetric response of a Bose-Fermi mixture to photoassociation. *Phys. Rev. A*, 81:011604, Jan 2010.
- [74] Y. Yu and K. Yang. Simulating the wess-zumino supersymmetry model in optical lattices. *Phys. Rev. Lett.*, 105:150605, Oct 2010.
- [75] F. Halzen and A.D. Martin. *Quarks and leptons: an introductory course in modern particle physics*. Wiley, 1984.
- [76] P. Langacker. *The Standard Model and Beyond*. Series in High Energy Physics, Cosmology and Gravitation. Taylor & Francis, 2011.
- [77] F. Englert and R. Brout. Broken symmetry and the mass of gauge vector mesons. *Phys. Rev. Lett.*, 13:321–323, Aug 1964.
- [78] Peter W. Higgs. Broken symmetries and the masses of gauge bosons. *Phys. Rev. Lett.*, 13:508–509, Oct 1964.
- [79] C. N. Yang and R. L. Mills. Conservation of isotopic spin and isotopic gauge invariance. *Phys. Rev.*, 96:191–195, Oct 1954.
- [80] J.D. Bjorken and S.D. Drell. *Relativistic quantum fields*. International series in pure and applied physics. McGraw-Hill, 1965.
- [81] C. Itzykson and J.B. Zuber. *Quantum field theory*. International series in pure and applied physics. McGraw-Hill International Book Co., 1980.
- [82] M.E. Peskin and D.V. Schroeder. *An Introduction to Quantum Field Theory*. Advanced book classics. Addison-Wesley Publishing Company, 1995.
- [83] P. Ramond. *Field Theory*. Frontiers in physics. Westview Press, 1997.
- [84] M. Srednicki. *Quantum Field Theory*. Cambridge University Press, 2007.
- [85] D. J. Gross and F. Wilczek. Ultraviolet behavior of non-Abelian gauge theories. *Phys. Rev. Lett.*, 30:1343–1346, Jun 1973.
- [86] J. D. Bjorken. Asymptotic sum rules at infinite momentum. *Phys. Rev.*, 179:1547–1553, Mar 1969.
- [87] J. D. Bjorken and E. A. Paschos. Inelastic electron-proton and gamma-proton scattering and the structure of the nucleon. *Phys. Rev.*, 185:1975–1982, Sep 1969.
- [88] K. G. Wilson. Confinement of quarks. *Phys. Rev. D*, 10(8):2445–2459, Oct 1974.
- [89] J. B. Kogut. An introduction to lattice gauge theory and spin systems. *Rev. Mod. Phys.*, 51(4):659–713, Oct 1979.
- [90] John B. Kogut. The lattice gauge theory approach to quantum chromodynamics. *Rev. Mod. Phys.*, 55:775–836, Jul 1983.
- [91] S. Aoki et al. Review of lattice results concerning low energy particle physics. *arXiv:1310.8555 [hep-lat]*, 2013.
- [92] Edward V. Shuryak. Quantum chromodynamics and the theory of superdense matter. *Physics Reports*, 61(2):71 – 158, 1980.
- [93] B. Svetitsky and L. G. Yaffe. Critical behavior at finite-temperature confinement transitions. *Nuclear Physics B*, 210(4):423 – 447, 1982.
- [94] L. McLerran. The physics of the quark-gluon plasma. *Rev. Mod. Phys.*, 58:1021–1064, Oct 1986.
- [95] B. Svetitsky. Symmetry aspects of finite-temperature confinement transitions. *Physics Reports*, 132(1):1 – 53, 1986.
- [96] A.M. Polyakov. Thermal properties of gauge fields and quark liberation. *Physics Letters B*, 72(4):477 – 480, 1978.
- [97] Leonard Susskind. Lattice models of quark confinement at high temperature. *Phys. Rev. D*, 20:2610–2618, Nov 1979.
- [98] Larry D. McLerran and Benjamin Svetitsky. A monte carlo study of su(2) yang-mills theory at finite temperature. *Physics Letters B*, 98(3):195 – 198, 1981.
- [99] Matthias Troyer and Uwe-Jens Wiese. Computational complexity and fundamental limitations

- to fermionic quantum monte carlo simulations. *Phys. Rev. Lett.*, 94:170201, May 2005.
- [100] J.B. Kogut and M.A. Stephanov. *The Phases of Quantum Chromodynamics: From Confinement to Extreme Environments*. Cambridge Monographs on Particle Physics, Nuclear Physics and Cosmology. Cambridge University Press, 2004.
- [101] K. Fukushima and T. Hatsuda. The phase diagram of dense QCD. *Reports on Progress in Physics*, 74(1):014001, 2011.
- [102] J. Schwinger. Gauge invariance and mass. *Phys. Rev.*, 125:397–398, Jan 1962.
- [103] J. Schwinger. Gauge invariance and mass. ii. *Phys. Rev.*, 128:2425–2429, Dec 1962.
- [104] J.H. Lowenstein and J.A. Swieca. Quantum electrodynamics in two dimensions. *Annals of Physics*, 68(1):172 – 195, 1971.
- [105] A. Casher, J. Kogut, and L. Susskind. Vacuum polarization and the absence of free quarks. *Phys. Rev. D*, 10:732–745, Jul 1974.
- [106] A. M. Polyakov. Quark confinement and topology of gauge theories. *Nucl. Phys. B*, 120(3):429 – 458, 1977.
- [107] T. Banks, R. Myerson, and J. Kogut. Phase transitions in Abelian lattice gauge theories. *Nucl. Phys. B*, 129(3):493 – 510, 1977.
- [108] S. D. Drell, H. R. Quinn, B. Svetitsky, and M. Weinstein. Quantum electrodynamics on a lattice: A Hamiltonian variational approach to the physics of the weak-coupling region. *Phys. Rev. D*, 19(2):619–638, Jan 1979.
- [109] S. Ben-Menahem. Confinement in compact QED for low couplings. *Phys. Rev. D*, 20(8):1923–1933, Oct 1979.
- [110] G. 't Hooft. A two-dimensional model for mesons. *Nucl. Phys. B*, 75(3):461 – 470, 1974.
- [111] C. G. Callan, N. Coote, and D. J. Gross. Two-dimensional Yang-Mills theory: A model of quark confinement. *Phys. Rev. D*, 13:1649–1669, Mar 1976.
- [112] K. Hornbostel, S. J. Brodsky, and H.-C. Pauli. Light-cone-quantized QCD in 1+1 dimensions. *Phys. Rev. D*, 41:3814–3821, Jun 1990.
- [113] A. Armoni, Y. Frishman, and J. Sonnenschein. Massless QCD2 from current constituents. *Nucl. Phys. B*, 596(12):459–470, February 2001.
- [114] E. Witten. Non-Abelian bosonization in two dimensions. *Comm. in Math. Phys.*, 92:455–472, 1984. 10.1007/BF01215276.
- [115] G.D. Date, Y. Frishman, and J. Sonnenschein. The spectrum of multiflavor QCD in two dimensions. *Nuclear Physics B*, 283(0):365–380, 1987.
- [116] Y. Frishman and J. Sonnenschein. Bosonization of colored flavored fermions and QCD in two dimensions. *Nuclear Physics B*, 294(0):801–812, 1987.
- [117] Y. Frishman and M. Karliner. Baryon wave functions and strangeness content in QCD2. *Nuclear Physics B*, 344(2):393–400, November 1990.
- [118] Y. Frishman and J. Sonnenschein. Bosonization and QCD in two dimensions. *Phys. Rep.*, 223(6):309–348, February 1993.
- [119] D. J. Gross, I. R. Klebanov, A. V. Matytsin, and A. V. Smilga. Screening versus confinement in 1 + 1 dimensions. *Nucl. Phys. B*, 461(12):109–130, February 1996.
- [120] A. Armoni, Y. Frishman, and J. Sonnenschein. The string tension in massive QCD2. *Phys. Rev. Lett.*, 80:430–433, Jan 1998.
- [121] E. Zohar, J. I. Cirac, and B. Reznik. Quantum simulations of gauge theories with ultracold atoms: Local gauge invariance from angular-momentum conservation. *Phys. Rev. A*, 88:023617, Aug 2013.
- [122] M. Hermele, M. P. A. Fisher, and L. Balents. Pyrochlore photons: The U(1) spin liquid in a $s=1/2$ three-dimensional frustrated magnet. *Phys. Rev. B*, 69(6):064404, Feb 2004.
- [123] H. P. Büchler, M. Hermele, S. D. Huber, Matthew P. A. Fisher, and P. Zoller. Atomic quantum simulator for lattice gauge theories and ring exchange models. *Phys. Rev. Lett.*, 95(4):040402, Jul 2005.
- [124] S. Tewari, V. W. Scarola, T. Senthil, and S. Das Sarma. Emergence of artificial photons in an optical lattice. *Phys. Rev. Lett.*, 97(20):200401, Nov 2006.
- [125] G. Szirmai, E. Szirmai, A. Zamora, and M. Lewenstein. Gauge fields emerging from time-reversal symmetry breaking for spin-5/2 fermions in a honeycomb lattice. *Phys. Rev. A*, 84:011611, Jul 2011.
- [126] E. Kapit and E. Mueller. Optical-lattice hamiltonians for relativistic quantum electrodynamics. *Phys. Rev. A*, 83:033625, Mar 2011.
- [127] E. Zohar and B. Reznik. Confinement and lattice quantum-electrodynamics electric flux tubes simulated with ultracold atoms. *Phys. Rev. Lett.*, 107:275301, Dec 2011.
- [128] E. Zohar, J. I. Cirac, and B. Reznik. Simulating compact quantum electrodynamics with ultracold atoms: Probing confinement and nonperturbative effects. *Phys. Rev. Lett.*,

- 109:125302, Sep 2012.
- [129] D. Horn. Finite matrix models with continuous local gauge invariance. *Physics Letters B*, 100(2):149 – 151, 1981.
- [130] P. Orland and D. Rohrlich. Lattice gauge magnets: Local isospin from spin. *Nuclear Physics B*, 338(3):647 – 672, 1990.
- [131] S. Chandrasekharan and U.-J. Wiese. Quantum link models: A discrete approach to gauge theories. *Nuclear Physics B*, 492(1 2):455 – 471, 1997.
- [132] D. Banerjee, M. Dalmonte, M. Müller, E. Rico, P. Stebler, U.-J. Wiese, and P. Zoller. Atomic quantum simulation of dynamical gauge fields coupled to fermionic matter: From string breaking to evolution after a quench. *Phys. Rev. Lett.*, 109:175302, Oct 2012.
- [133] E. Zohar, J. I. Cirac, and B. Reznik. Simulating (2+1)-dimensional lattice QED with dynamical matter using ultracold atoms. *Phys. Rev. Lett.*, 110:055302, Jan 2013.
- [134] D. Marcos, P. Rabl, E. Rico, and P. Zoller. Superconducting circuits for quantum simulation of dynamical gauge fields. *Phys. Rev. Lett.*, 111:110504, Sep 2013.
- [135] D. Marcos, P. Widmer, E. Rico, M. Hafezi, P. Rabl, U.-J. Wiese, and P. Zoller. Two-dimensional lattice gauge theories with superconducting quantum circuits. *Annals of Physics*, 351(0):634 – 654, 2014.
- [136] P. Hauke, D. Marcos, M. Dalmonte, and P. Zoller. Quantum simulation of a lattice schwinger model in a chain of trapped ions. *Phys. Rev. X*, 3:041018, Nov 2013.
- [137] L. Tagliacozzo, A. Celi, A. Zamora, and M. Lewenstein. Optical Abelian lattice gauge theories. *Annals of Physics*, 330(0):160 – 191, 2013.
- [138] B. Douçot, L. B. Ioffe, and J. Vidal. Discrete non-Abelian gauge theories in Josephson-junction arrays and quantum computation. *Phys. Rev. B*, 69:214501, Jun 2004.
- [139] S. Notarnicola, E. Ercolessi, P. Facchi, G. Marmo, S. Pascazio, and F.V. Pepe. Discrete abelian gauge theories for quantum simulations of qed. *arXiv:1503.04340 [quant-ph]*, 2015.
- [140] M. Mathur. Harmonic oscillator pre-potentials in SU (2) lattice gauge theory. *Journal of Physics A: Mathematical and General*, 38(46):10015, 2005.
- [141] M. Mathur. Loop states in lattice gauge theory. *Physics Letters B*, 640:292–296, 2006.
- [142] M. Mathur. Loop approach to lattice gauge theories. *Nuclear Physics B*, 779:32–62, 2007.
- [143] R. Anishetty, M. Mathur, and I. Raychowdhury. Prepotential formulation of SU (3) lattice gauge theory. *J. of Phys. A: Math. and Th.*, 43(3):035403, 2010.
- [144] R. Brower, S. Chandrasekharan, and U.-J. Wiese. QCD as a quantum link model. *Phys. Rev. D*, 60:094502, Sep 1999.
- [145] R. Brower, S. Chandrasekharan, S. Riederer, and U.-J. Wiese. D-theory: field quantization by dimensional reduction of discrete variables. *Nuclear Physics B*, 693(13):149 – 175, 2004.
- [146] E. Zohar, J. I. Cirac, and B. Reznik. Cold-atom quantum simulator for SU(2) yang-mills lattice gauge theory. *Phys. Rev. Lett.*, 110:125304, Mar 2013.
- [147] D. Banerjee, M. Bögli, M. Dalmonte, E. Rico, P. Stebler, U.-J. Wiese, and P. Zoller. Atomic quantum simulation of U(n) and SU(n) non-Abelian lattice gauge theories. *Phys. Rev. Lett.*, 110:125303, Mar 2013.
- [148] P. Orland. A reintroduction of dynamical SU(2) gauge fields in hubbard models. *arXiv:1207.0455 [cond-mat.str-el]*, 2012.
- [149] L. Tagliacozzo, A. Celi, P. Orland, and M. Lewenstein. Simulations of non-Abelian gauge theories with optical lattices. *Nat. Commun.*, 4, 2013.
- [150] A. Mezzacapo, E. Rico, C. Sabín, I.L. Egusquiza, L. Lamata, and E. Solano. Non-abelian lattice gauge theories in superconducting circuits. *arXiv:1505.04720 [quant-ph]*, 2015.
- [151] K. Stannigel, P. Hauke, D. Marcos, M. Hafezi, S. Diehl, M. Dalmonte, and P. Zoller. Constrained dynamics via the zeno effect in quantum simulation: Implementing non-abelian lattice gauge theories with cold atoms. *Phys. Rev. Lett.*, 112:120406, Mar 2014.
- [152] U.-J. Wiese. Ultracold quantum gases and lattice systems: quantum simulation of lattice gauge theories. *Annalen der Physik*, 525(10-11):777–796, 2013.
- [153] M. Creutz. *Quarks, Gluons and Lattices*. Cambridge Monographs on Mathematical Physics. Cambridge University Press, 1983.
- [154] I. Montvay and G. Munster. *Quantum Fields on a Lattice*. Cambridge Monographs on Mathematical Physics. Cambridge University Press, 1997.
- [155] J. Smit. *Introduction to Quantum Fields on a Lattice*. Cambridge Lecture Notes in Physics. Cambridge University Press, 2002.
- [156] H.J. Rothe. *Lattice Gauge Theories: An Introduction*. Lattice Gauge Theories: An Introduction. World Scientific, 2005.
- [157] J. Kogut and L. Susskind. Hamiltonian formulation of Wilson’s lattice gauge theories. *Phys. Rev. D*, 11(2):395–408, Jan 1975.

- [158] A. M. Polyakov. *Gauge Fields and Strings*. Contemporary concepts in physics. Taylor & Francis, 1987.
- [159] Leonard Susskind. Lattice fermions. *Phys. Rev. D*, 16:3031–3039, Nov 1977.
- [160] L. H. Karsten and J. Smith. Lattice fermions: Species doubling, chiral invariance and the triangle anomaly. *Nuclear Physics B*, 183(12):103 – 140, 1981.
- [161] G. 't Hooft. On the phase transition towards permanent quark confinement. *Nuclear Physics B*, 138(1):1–25, June 1978.
- [162] D. Horn, M. Weinstein, and S. Yankielowicz. Hamiltonian approach to $Z(N)$ lattice gauge theories. *Phys. Rev. D*, 19:3715–3731, Jun 1979.
- [163] Erez Zohar and Michele Burrello. Formulation of lattice gauge theories for quantum simulations. *Phys. Rev. D*, 91:054506, Mar 2015.
- [164] L.D. Landau and E.M. Lifshitz. *Quantum Mechanics: Non-Relativistic Theory*. Teoreticheskiiĭ aĭzĭ fizika. Elsevier Science, 1981.
- [165] M.E. Rose. *Elementary Theory of Angular Momentum*. Dover books on physics and chemistry. Dover, 1995.
- [166] A.R. Edmonds. *Angular Momentum in Quantum Mechanics*. Investigations in Physics Series. Princeton University Press, 1996.
- [167] C.J. Hamer. Lattice model calculations for $SU(2)$ yang-mills theory in $1 + 1$ dimensions. *Nucl. Phys. B*, 121(1):159 – 175, 1977.
- [168] E. Fradkin and L. Susskind. Order and disorder in gauge systems and magnets. *Phys. Rev. D*, 17:2637–2658, May 1978.
- [169] S. Elitzur, R. B. Pearson, and J. Shigemitsu. Phase structure of discrete abelian spin and gauge systems. *Phys. Rev. D*, 19:3698–3714, Jun 1979.
- [170] G. Bhanot and Michael Creutz. Phase diagram of $Z(N)$ and $U(1)$ gauge theories in three dimensions. *Phys. Rev. D*, 21:2892–2902, May 1980.
- [171] T. Banks, L. Susskind, and J. Kogut. Strong-coupling calculations of lattice gauge theories: $(1 + 1)$ -dimensional exercises. *Phys. Rev. D*, 13:1043–1053, Feb 1976.
- [172] M.C. Bañuls, K. Cichy, J.I. Cirac, and K. Jansen. The mass spectrum of the schwinger model with matrix product states. *Journal of High Energy Physics*, 2013(11), 2013.
- [173] M.C. Bañuls, K. Cichy, J.I. Cirac, K. Jansen, and H. Saito. *Proc. Sci. LATTICE 2013*, 332, 2013.
- [174] Stefan Kühn, J. Ignacio Cirac, and Mari-Carmen Bañuls. Quantum simulation of the schwinger model: A study of feasibility. *Phys. Rev. A*, 90:042305, Oct 2014.
- [175] Boye Buyens, Jutho Haegeman, Karel Van Acoleyen, Henri Verschelde, and Frank Verstraete. Matrix product states for gauge field theories. *Phys. Rev. Lett.*, 113:091601, Aug 2014.
- [176] Hana Saito, Mari Carmen Bañuls, Krzysztof Cichy, J. Ignacio Cirac, and Karl Jansen. The temperature dependence of the chiral condensate in the schwinger model with matrix product states. *arXiv:1412.0596; PoS(LATTICE2014)302*, 2014.
- [177] M. C. Bañuls, K. Cichy, J. I. Cirac, K. Jansen, and H. Saito. Thermal evolution of the schwinger model with matrix product operators. *arXiv:1505.00279*, 2015.
- [178] T. Pichler, M. Dalmonte, E. Rico, P. Zoller, and S. Montangero. Real-time dynamics in $u(1)$ lattice gauge theories with tensor networks. *arXiv:1505.04440 [cond-mat.quant-gas]*, 2015.
- [179] D. M. Stamper-Kurn and W. Ketterle. *Spinor Condensates and Light Scattering from Bose-Einstein Condensates*, pages 137–217. Springer, New York, 2001.
- [180] C. Pethick and H. Smith. *Bose-Einstein Condensation in Dilute Gases*. Cambridge University Press, 2002.
- [181] H. Feshbach. Unified theory of nuclear reactions. *Annals of Physics*, 5(4):357 – 390, 1958.
- [182] P. O. Fedichev, Yu. Kagan, G. V. Shlyapnikov, and J. T. M. Walraven. Influence of nearly resonant light on the scattering length in low-temperature atomic gases. *Phys. Rev. Lett.*, 77(14):2913–2916, Sep 1996.
- [183] J. L. Bohn and P. S. Julienne. Prospects for influencing scattering lengths with far-off-resonant light. *Phys. Rev. A*, 56(2):1486–1491, Aug 1997.
- [184] S. Inouye, M. R. Andrews, J. Stenger, H.-J. Miesner, D. M. Stamper-Kurn, and W. Ketterle. Observation of feshbach resonances in a bose-einstein condensate. *Nature*, 392(6672):151–154, March 1998.
- [185] S. L. Cornish, N. R. Claussen, J. L. Roberts, E. A. Cornell, and C. E. Wieman. Stable ^{85}Rb bose-einstein condensates with widely tunable interactions. *Phys. Rev. Lett.*, 85:1795–1798, Aug 2000.
- [186] F. K. Fatemi, K. M. Jones, and P. D. Lett. Observation of optically induced Feshbach resonances in collisions of cold atoms. *Phys. Rev. Lett.*, 85(21):4462–4465, Nov 2000.
- [187] C. Chin, R. Grimm, P. Julienne, and E. Tiesinga. Feshbach resonances in ultracold gases. *Rev.*

- Mod. Phys.*, 82:1225–1286, Apr 2010.
- [188] S. Blatt, T. L. Nicholson, B. J. Bloom, J. R. Williams, J. W. Thomsen, P. S. Julienne, and J. Ye. Measurement of optical Feshbach resonances in an ideal gas. *Phys. Rev. Lett.*, 107:073202, Aug 2011.
- [189] W. S. Bakr, J. I. Gillen, A. Peng, S. Folling, and M. Greiner. A quantum gas microscope for detecting single atoms in a Hubbard-regime optical lattice. *Nature*, 462(7269):74–77, November 2009.
- [190] C. Weitenberg, M. Endres, J. F. Sherson, M. Cheneau, P. Schausz, T. Fukuhara, I. Bloch, and S. Kuhr. Single-spin addressing in an atomic Mott insulator. *Nature*, 471(7338):319–324, March 2011.
- [191] Maxwell F. Parsons, Florian Huber, Anton Mazurenko, Christie S. Chiu, Widagdo Setiawan, Katherine Wooley-Brown, Sebastian Blatt, and Markus Greiner. Site-resolved imaging of fermionic ${}^6\text{Li}$ in an optical lattice. *Phys. Rev. Lett.*, 114:213002, May 2015.
- [192] P. Wurtz, T. Langen, T. Gericke, A. Koglbauer, and H. Ott. Experimental demonstration of single-site addressability in a two-dimensional optical lattice. *Phys. Rev. Lett.*, 103:080404, Aug 2009.
- [193] C E Soliveréz. An effective Hamiltonian and time-independent perturbation theory. *J. of Phys. C: Solid State Phys.*, 2(12):2161, 1969.
- [194] C. Cohen-Tannoudji, G. Grynberg, and J. Dupont-Roc. *Atom-Photon Interactions: Basic Processes and Applications*. Wiley, New York, 1992.
- [195] L. Mazza, M. Rizzi, M. Lewenstein, and J. I. Cirac. Emerging bosons with three-body interactions from spin-1 atoms in optical lattices. *Phys. Rev. A*, 82:043629, Oct 2010.
- [196] K Kasamatsu, I. Ichinose, and T. Matsui. Atomic quantum simulation of the lattice gauge-Higgs model: Higgs couplings and emergence of exact local gauge symmetry. *Phys. Rev. Lett.*, 111:115303, Sep 2013.
- [197] Y. Kuno, K. Kasamatsu, Y. Takahashi, I. Ichinose, and Matsui T. A formulation of lattice gauge theories for quantum simulations. *arXiv preprint arXiv:1412.7605*, 2014.
- [198] P. Jordan. Der Zusammenhang der symmetrischen und linearen Gruppen und das Mehrkoerperproblem. *Z. Phys.*, 94(7-8):531, 1935.
- [199] J. Schwinger. US atomic energy commission report nyo-3071. *US Atomic Energy Commission Report NYO-3071*, 1952.
- [200] E. Zohar and B. Reznik. Topological Wilson-loop area law manifested using a superposition of loops. *New J. Phys.*, 15(4):043041, 2013.
- [201] H. B. Nielsen and J. G. Taylor. Field theories without fundamental gauge symmetries [and discussion]. *Philosophical Transactions of the Royal Society of London A: Mathematical, Physical and Engineering Sciences*, 310(1512):261–272, 1983.
- [202] N. F. Ramsey. Experiments with separated oscillatory fields and hydrogen masers. *Rev. Mod. Phys.*, 62:541–552, Jul 1990.
- [203] E. Rico, T. Pichler, M. Dalmonte, P. Zoller, and S. Montangero. Tensor networks for lattice gauge theories and atomic quantum simulation. *Phys. Rev. Lett.*, 112:201601, May 2014.
- [204] L. Tagliacozzo, A. Celi, and M. Lewenstein. Tensor networks for lattice gauge theories with continuous groups. *Phys. Rev. X*, 4:041024, Nov 2014.
- [205] J. Haegeman, K. Van Acoleyen, N. Schuch, J. I. Cirac, and F. Verstraete. Gauging quantum states: From global to local symmetries in many-body systems. *Phys. Rev. X*, 5:011024, Feb 2015.
- [206] P. Silvi, E. Rico, T. Calarco, and S. Montangero. Lattice gauge tensor networks. *New Journal of Physics*, 16(10):103015, 2014.
- [207] S. Kühn, E. Zohar, J.I. Cirac, and M.C. Bañuls. Non-abelian string breaking phenomena with matrix product states. *arXiv:1505.04441 [hep-lat]*, 2015.
- [208] E. Zohar, M. Burrello, T. B. Wahl, and J. I. Cirac. Fermionic projected entangled pair states and local $u(1)$ gauge theories. *arXiv:1507.08837*, 2015.